A Theoretical Model for S_N1 Ionic Dissociation in Solution. 1. Activation Free Energetics and Transition-State Structure

Hyung J. Kim[†] and James T. Hynes*

Contribution from the Department of Chemistry and Biochemistry, University of Colorado, Boulder, Colorado 80309-0215. *Received April 3, 1991*

Abstract: The rate-determining ionic dissociation $RX \rightarrow R^+ + X^-$ for S_N1 reactions in a polar solvent is examined theoretically. These unimolecular dissociations involve critical and extensive solvent stabilization of the ionic state compared to the covalent state to induce an electronic curve crossing to allow the heterolysis. Our approach is via a nonlinear Schrödinger equation theory recently developed to account for the mutual influence of solute electronic structure and solvent polarization—both equilibrium and nonequilibrium. The theory deals quantitatively with the competition between the electronic coupling between covalent and ionic valence bond states—which tends to mix these states—and solvation which tends to localize the system in one of them. Novel aspects of the theory as applied to S_N1 ionizations include removal of the restriction of the pioneering Ogg–Polanyi solvent-equilibrated diabatic curve intersection approach—which predicts an invariant 50% ionic character of the transition state, connection to (and contrasts with) an electron-transfer perspective for the reaction, and exposure of the role of the solvent electronic polarization in stabilizing the delocalized transition state. By adopting a simple model for *tert*-butyl chloride in a dielectric continuum model for solvents of differing polarity, we implement the theory to obtain a two-dimensional free energy surface in terms of the R–X separation r and a solvent coordinate s, which gauges the nonequilibrium solvent orientational polarization. Along s, a single stable well potential results, in contrast to activated electron-transfer reactions—this clarifies the issue of electron transfer versus electron shift in the reaction. One measure of this contrast is the predicted lack of applicability of Marcus activation–reaction free energy relations for this reaction class. Activation free energy barriers for heterolysis are calculated, compared with experimental results, and the trends are examined and explained. The change in the ionization transition-state structure with solvent polarity is also analyzed. The ionic character of the transition state is found to decrease with increasing solvent polarity; the transition state becomes *less* ionic for more polar solvents, in direct contrast to prevalent notions. The activation free energy $\Delta G^{\ddagger}$ itself decreases with increasing solvent polarity; this trend is in accord with experiment and standard conceptions. However, the dominant *source* of this trend of $\Delta G^{\ddagger}$ with solvent polarity—the *variation of the electronic coupling* between the covalent and ionic states—contrasts fundamentally with that conventionally envisioned via, e.g., a Hughes–Ingold perspective. In addition, our analytic relationship connecting the activation free energy and the solvent polarity differs markedly from that often used to determine the transition-state ionic character. Solvent polarity dependence of a Brønsted coefficient is suggested as an experimental probe of the new perspective. Finally, locally stable ion pair products in weakly polar and nonpolar solvents are found and discussed.

1. Introduction

It is well-known that alkyl (and other) organic halides such as *tert*-butyl chloride (*t*-BuCl) undergo a unimolecular ionic dissociation

$$RX \rightarrow R^+ + X^- \qquad (1.1)$$

in a polar solvent as the rate-determining step in S_N1 reactions.[1-16] The nature of this process has been the object of manifold studies, including early seminal investigations by Hughes and Ingold,[1] Ogg, Evans, and Polanyi,[2] and Grunwald, Winstein, and their co-workers,[3] together with significant contributions by many others continuing to the present.[4-23] Typical magnitudes of the ionization potential for the organic species R and of the electron affinity for the halogen atom X are such that the former exceeds the latter, and the ground state in vacuum in consequence is mainly a covalent state. In a polar solvent, however, the ionic state is stabilized with respect to the covalent state and thus RX can dissociate into ions. This important reaction class thus provides an arena in which the solvent is critical in determining the reaction pathway.

Some basic features of this ionic dissociation were qualitatively explained long ago by Ogg, Polanyi, Evans, and their co-workers[2] in terms of electronic curve crossing between the pure covalent state and the solvated pure ionic state.[2,23,24] Implicit assumptions made there include the supposition that equilibrium solvation of the solute applies during the entire dissociation, thus ensuring the maximum stabilization for the pure ionic state due to solvation. However, from the examples of electron-transfer reactions and other charge transfer and shift reactions in solution, one can easily imagine that nonequilibrium solvation may play an important role in both the reaction path and rate. These features were first examined for S_N1 ionizations by Zichi and Hynes[17] in a model study employing the Grote–Hynes theory[25] and subsequently by Lee and Hynes[18b] via a solution-phase reaction path Hamiltonian

[†] Present address: Dept. of Chemistry, Carnegie Mellon University, Pittsburgh, PA 15213-3890.

(1) (a) Gleave, J. L.; Hughes, E. D.; Ingold, C. K. *J. Chem. Soc.* (*London*) **1935**, 236. (b) Hughes, E. D.; Ingold, C. K. *J. Chem. Soc.* (*London*) **1935**, 244. (c) Hughes, E. D.; Ingold, C. K. *Trans. Faraday Soc.* **1941**, *37*, 657. (d) Dostrovski, I.; Hughes, E. D.; Ingold, C. K. *J. Chem. Soc.* (*London*) **1946**, 173. (e) Gelles, E.; Hughes, E. D.; Ingold, C. K. *J. Chem. Soc.* (*London*) **1954**, 2918. (f) Ingold, C. K. *Proc. Chem. Soc.* **1957**, 279. (g) Ingold, C. K. *Proc. Chem. Soc.* **1962**, 265. (h) Ingold, C. K. *Structure and Mechanism in Organic Chemistry*, 22nd ed.; Cornell University: Ithaca, NY, 1969.

(2) (a) Ogg, R. A., Jr.; Polanyi, M. *Trans. Faraday Soc.* **1935**, *31*, 604. See, also: (b) Baughan, E. C.; Evans, M. G.; Polanyi, M. *Trans. Faraday Soc.* **1941**, *37*, 377. (c) Evans, A. G. *Trans. Faraday Soc.* **1946**, *42*, 719.

(3) (a) Grunwald, E.; Winstein, S. *J. Am. Chem. Soc.* **1948**, *70*, 846. (b) Winstein, S.; Grunwald, E.; Jones, H. W. *J. Am. Chem. Soc.* **1951**, *73*, 2700. (c) Winstein, S.; Clippinger, E.; Fainberg, A. H.; Robinson, G. C. *J. Am. Chem. Soc.* **1954**, *76*, 2597. (d) Fainberg, A. H.; Winstein, S. *J. Am. Chem. Soc.* **1956**, *78*, 2770. (e) Winstein, S.; Fainberg, A. H. *J. Am. Chem. Soc.* **1957**, *79*, 5937. (f) Cocivera, M.; Winstein, S. *J. Am. Chem. Soc.* **1963**, *85*, 1702.

(4) (a) Swain, C. G. *J. Am. Chem. Soc.* **1948**, *70*, 1119. (b) Swain, C. G.; Mosely, R. B. *J. Am. Chem. Soc.* **1955**, *77*, 3727.

(5) Doering, W. E.; Zeiss, H. H. *J. Am. Chem. Soc.* **1953**, *75*, 4733.

(6) Streitwieser, A., Jr. *Solvolytic Displacement Reactions*; McGraw-Hill: New York, 1962.

(7) (a) Robertson, R. E.; Heppolette, R. L.; Scott, J. M. W. *Can. J. Chem.* **1959**, *37*, 803. (b) Laughton, P. M.; Roberson, R. E. In *Solute–Solvent Interactions*; Coetzee, J. F., Ritchie, C. D., Eds.; M. Dekker: New York, 1969. (c) Blandamer, M. J.; Scott, J. M. W.; Robertson, R. E. *Prog. Phys. Org. Chem.* **1985**, *15*, 149.

(8) (a) Arnett, E. M.; McKelvey, D. R. *Rec. Chem. Prog.* **1965**, *26*, 185. (b) Arnett, E. M.; Bentrude, W. G.; Dubbleby, P. M. *J. Am. Chem. Soc.* **1965**, *87*, 2048. (c) Arnett, E. M. In *Physico-Chemical Processes in Mixed Aqueous Solvents*; Franks, F., Ed.; American Elsevier: New York, 1967. (d) Arnett, E. M.; Petro, C.; Schleyer, P. v. R. *J. Am. Chem. Soc.* **1979**, *101*, 522.

(9) Raber, D. J.; Harris, J. M.; Schleyer, P. v. R. In *Ions and Ion Pairs in Organic Reactions*; Szwarc, M., Ed.; Wiley: New York, 1974; Vol. 2.

(10) (a) Ritchie, C. D. In *Solute–Solvent Interactions*; Coetzee, J. F., Ritchie, C. D., Eds.; M. Dekker: New York, 1969. (b) Ritchie, C. D. *Can. J. Chem.* **1986**, *64*, 2239. (c) In *Nucleophilicity*; Harris, J. M., McManus, S. P., Eds.; ACS: Washington, D.C., 1987.

0002-7863/92/1514-10508$03.00/0

formulation.[18a] However, the explicit quantum chemical, electronic structure aspects of the problem were in effect bypassed, by adopting certain models for the evolving solute charge distribution.

In this paper and the following paper in this issue,[26] hereafter referred to as part 2, we construct a theoretical framework for S_N1 ionic dissociations—to describe the transition-state character and its free energetic properties, the reaction path, and nonequilibrium solvation effects on the rate—beginning with a description of the solute electronic structure in the presence of the solvent electronic and orientational polarizations. For this purpose, we employ a nonlinear Schrödinger equation formalism in a two-valence bond-state basis that we have recently developed[27] to describe solute electronic structure in solution. This formalism goes beyond related equilibrium reaction field theories[28,29] in that it applies when the surrounding solvent either is or is not in equilibrium with the solute quantum charge distribution[17,18,30] and also in its attention to issues of the time scales of the solute and solvent electrons.[27,31,32] We will find that the electronic structure aspects of the problem are critical for understanding the S_N1 ionization. Of essential importance is the competition between the electronic coupling—which favors a delocalized transition state of 50% ionic character—and the solvation free energy—which favors a localized electronic character of the transition state that is purely ionic. A further indication of the importance of the electronic coupling is that we will find that its variation governs the trend with solvent polarity of the reaction activation free energy; this distinctly contrasts with the standard Hughes–Ingold perspective,[1-16] in which that trend is supposed to arise directly from changes in the solvation stabilization of the transition state.

The solvent is described at the dielectric continuum level. While this is automatically suspect at the molecular level,[30,33,34] the activation free energies that we estimate for *t*-BuCl ionization in various solvents are in reasonable accord with experimental estimates. This also helps justify, to a degree, the lowest level two state electronic structure treatment. But even with this semiquantitative success, our treatment is primarily intended to provide a theoretical framework for comprehension of the ionization process and the critical factors which govern both its route and rate. To this end, we extensively employ a two-dimensional free energy surface[18,35] in the RX nuclear separation coordinate and a collective solvent coordinate to examine and quantify the "polymolecular"[36] solvent-effected ionization process. In this paper, attention is mainly focused on one-dimensional projections for this surface, while the two-dimensional character is fully exploited in part 2[26] to examine the reaction path. We also couch a large portion of our analysis in terms of quantities—such as reorganization and solvation free energies—which have significance beyond the confines of a continuum solvent description.

To be sure, the ionization step eq 1.1 is but one component—albeit the rate-limiting one—in overall unimolecular S_N1 ionic reaction schemes accounting for the mechanistic details of,[1-16] e.g.

$$RX \rightarrow R^+ + X^- \quad \text{(slow)}$$

$$R^+ + X^- + R'OH \rightarrow ROR' + HX \quad \text{(fast)} \quad (1.2)$$

in the case of alcoholysis. Here we focus our attention solely on the ionization step and do not address the myriad issues[1-16] of the subsequent fate of the ions or ion pairs produced.[37] However,

(11) (a) Abraham, M. H. *J. Chem. Soc., Perkin Trans. 2* **1972**, 1343. (b) *Prog. Phys. Org. Chem.* **1974**, *11*, 1. (c) Abraham, M. H.; Abraham, R. J. *J. Chem. Soc., Perkin Trans. 2* **1974**, 47. (d) Abraham, M. H. In *Advances in Solution Chemistry*; Bertini, I., Lunazzi, L., Dei, A., Eds.; Plenum: New York, 1981. (e) Abraham, M. H.; Grellier, P. L.; Nasehzadeh, A.; Walker, R. A. C. *J. Chem. Soc., Perkin Trans. 2* **1988**, 1717.

(12) (a) Koppel, I. A.; Palm, V. A. *Org. React. (Tartu)* **1969**, *6*, 213. (b) Ponomareva, E. A.; Kulik, N. I.; Dvorko, G. F. *Org. React. (Tartu)* **1974**, *11*, 333.

(13) Kevill, D. N.; Dorsey, J. E. *Chem. Ind.* **1967**, 2174.

(14) Cremaschi, P.; Gamba, A.; Simonetta, M. *J. Chem. Soc., Perkin Trans. 2* **1977**, 162. Revettlat, J. A.; Oliva, A.; Bertrán, J. *J. Chem. Soc., Perkin Trans. 2* **1984**, 815. Yamabe, S.; Yamabe, E.; Minato, T. *J. Chem. Soc., Perkin Trans. 2* **1983**, 1881. Salem, L. *Electrons in Chemical Reactions*; Wiley: New York, 1982.

(15) (a) Symons, M. C. R. *J. Chem. Soc., Chem. Commun.* **1978**, 418. (b) Blandamer, M. J.; Burgess, J.; Duce, P. P.; Symons, M. C. R.; Robertson, R. E.; Scott, J. M. W. *J. Chem. Res. (S)* **1982**, 130.

(16) (a) For a recent review, see: Dvorko, G. F., Ponomareva, E. A.; Kulik, N. I. *Russ. Chem. Rev.* **1984**, *53*, 547. (b) See also: Richard, J. P. *Adv. Carbocation Chem.* **1989**, *1*, 121. Okamoto, K. *Adv. Carbocation Chem.* **1989**, *1*, 171.

(17) Zichi, D. A.; Hynes, J. T. *J. Chem. Phys.* **1988**, *88*, 2513.

(18) (a) Lee, S.; Hynes, J. T. *J. Chem. Phys.* **1988**, *88*, 6853. (b) Lee, S.; Hynes, J. T. *J. Chem. Phys.* **1988**, *88*, 6863.

(19) (a) Pross, A.; Shaik, S. S. *Acc. Chem. Res.* **1983**, *16*, 363. (b) Pross, A.; Shaik, S. S. *Tetrahedron Lett.* **1982**, *23*, 5467.

(20) (a) Pross, A. *Adv. Phys. Org. Chem.* **1985**, *21*, 99. (b) Pross, A. *Acc. Chem. Res.* **1985**, *18*, 212.

(21) (a) Shaik, S. S. *Prog. Phys. Org. Chem.* **1985**, *15*, 197. (b) Shaik, S. S. *J. Org. Chem.* **1987**, *52*, 1563.

(22) Kochi, J. K. *Angew. Chem., Int. Ed. Engl.* **1988**, *27*, 1227.

(23) (a) Warshel, A.; Weiss, R. M. *J. Am. Chem. Soc.* **1980**, *102*, 6218. (b) Warshel, A. *J. Phys. Chem.* **1982**, *86*, 2218. (c) Warshel, A. *Acc. Chem. Res.* **1981**, *14*, 284. In *The Enzyme Catalysis Process: Energetics, Mechanism, and Dynamics*; Cooper, A., Houben, J. L., Chien, L. C., Eds.; Plenum: New York, 1989.

(24) For other examples of solvent-assisted curve crossing, see, for example: Salem, L. *Science* **1976**, *191*, 822.

(25) Grote, R. F.; Hynes, J. T. *J. Chem. Phys.* **1980**, *73*, 2715. See, also: Hynes, J. T. In *The Theory of Chemical Reaction Dynamics*; Baer, M., Ed.; CRC Press: Boca Raton, FL, 1985; Vol. 4.

(26) Kim, H. J.; Hynes, J. T. *J. Am. Chem. Soc.* the following paper in this issue.

(27) Kim, H. J.; Hynes, J. T. *J. Chem. Phys.* **1992**, *96*, 5088.

(28) (a) Beens, H.; Weller, A. *Chem. Phys. Lett.* **1969**, *3*, 666. In *Organic Molecular Photophysics*; Birks, J. B., Ed.; Wiley: London, 1975, Vol. 2. (b) Newton, M. D. *J. Chem. Phys.* **1973**, *58*, 5833. *J. Phys. Chem.* **1975**, *79*,2795. (c) Yomosa, S. *J. Phys. Soc. Jpn.* **1973**, *35*, 1738; **1974**, *36*, 1655; **1978**, *44*, 602. (d) Tapia, O.; Goscinski, O. *Mol. Phys.* **1975**, *29*, 1653. Tapai, O. In *Quantum Theory of Chemical Reactions*; Daudel, R., Pullman, A., Salem, L., Veillard, A., Eds.; Reidel: Dordrecht, 1980; Vol. 2. *J. Mol. Struct.* **1991**, *226*, 59. (e) Rivail, J.-L.; Rinaldi, D. *Chem. Phys.* **1976**, *18*, 233. Rivial, J.-L. In *Chemical Reactivity in Liquids*; Moreau, M., Turq, P., Eds.; Plenum: New York, 1988. (f) Ghio, C.; Scrocco, E.; Tomasi, J. In *Environmental Effects on Molecular Structure and Properties*; Pullman, B., Ed.; Reidel: Dordrecht, 1976. Miertuš, S.; Scrocco, E.; Tomasi, J. *Chem. Phys.* **1981**, *55*, 117; Miertuš, S.; Tomasi, J. *Chem. Phys.* **1982**, *65*, 239. (g) Karlström, G. *J. Phys. Chem.* **1988**, *92*, 1315. (h) Mikkelsen, K. V.; Dalgaard, E.; Swanstrøm, P. *J. Phys. Chem.* **1987**, *91*, 3081. Mikkelsen, K. V.; Ratner, M. A. *Int. J. Quantum Chem. Quantum Chem. Symp.* **1988**, *22*, 707. (i) Karelson, M.; Tamm, T.; Katritzky, A. R.; Szafran, M.; Zerner, M. C. *Int. J. Quantum Chem.* **1990**, *37*, 1. (j) Wong, M. W.; Wiberg, K. B.; Frisch, M. *J. Chem. Phys.* **1991**, *95*, 8991. Wong, M. W.; Frisch, M.; Wiberg, K. B. *J. Am. Chem. Soc.* **1991**, *113*, 4776.

(29) (a) Hylton, J.; Christoffersen, R. E.; Hall, G. G. *Chem. Phys. Lett.* **1974**, *26*, 501. Hylton McCreery, J.; Christoffersen, R. E.; Hall, G. G. *J. Am. Chem. Soc.* **1976**, *98*, 7191. (b) Thole, B. T.; van Duijnen, P. T. *Theor. Chim. Acta* **1980**, *55*, 307. *Chem. Phys.* **1981**, *71*, 211. (c) See, also: Ángyán, J. G.; Jansen, G. *Chem. Phys. Lett.* **1990**, *175*, 313. (d) When both the solvent orientational and electronic polarizations are in equilibrium with the solute charge (i.e., when equilibrium solvation occurs), the Born–Oppenheimer approximation does not lead to Onsager's equilibrium reaction field, widely used in calculating the equilibrium free energy in solution (see refs 27 and 30a).

(30) In the context of self-consistent field approximation, see: (a) Kim, H. J.; Hynes, J. T. *J. Chem. Phys.* **1990**, *93*, 5194. (b) Kim, H. J.; Hynes, J. T. *J. Chem. Phys.* **1990**, *93*, 5211. (c) Kim, H. J.; Hynes, J. T. *J. Phys. Chem.* **1990**, *94*, 2736. (d) Kim, H. J.; Hynes, J. T. *Int. J. Q. Chem. Quantum Chem. Symp.* **1990**, *24*, 821.

(31) Gehlen, J.; Chandler, D.; Kim, H. J.; Hynes, J. T. *J. Phys. Chem.* **1992**, *96*, 1748.

(32) Marcus, R. A. *J. Phys. Chem.* **1992**, *96*, 1753.

(33) Morita, T.; Ladanyi, B. M.; Hynes, J. T. *J. Phys. Chem.* **1989**, *93*, 1386.

(34) The bulky butyl appendages of the *t*-Bu group assist in minimizing nucleophilic participation of the solvent,[5,12] an effect certainly not accounted for in a continuum solvent model.

(35) (a) van der Zwan, G.; Hynes, J. T. *J. Chem. Phys.* **1982**, *76*, 2993. (b) van der Zwan, G.; Hynes, J. T. *J. Chem. Phys.* **1983**, *78*, 4174. (c) van der Zwan, G.; Hynes, J. T. *Chem. Phys.* **1984**, *90*, 21.

(36) (a) Farinacci, N. T.; Hammett, L. P. *J. Am. Chem. Soc.* **1937**, *59*, 2542. (b) Steigman, J.; Hammett, L. P. *J. Am. Chem. Soc.* **1937**, *59*, 2536. (c) Hammett, L. P. *Physical Organic Chemistry*; McGraw-Hill: New York, 1940.

(37) In addition, we do not here explicitly comment on electrophile–nucleophile combination reactions,[10] which in the ionic case bear a reverse reaction relation to many of the issues we address.

a brief discussion is given of the ion pairs generated in ionizations in very weakly polar and nonpolar solvents—a conventionally improbable but nonetheless fertile reaction arena identified quite some time ago by Ingold.[1f] We do however need to briefly address a related issue at the outset to place our work in perspective. This is the unimolecular elimination E1 mechanism[1,11,13,16] by which, e.g., an alkyl halide eliminates the hydrohalic acid to produce an alkene

$$Me_2CH_3CX \rightarrow Me_2C{=}CH_2 + HX \qquad (1.3)$$

In polar and nonpolar aprotic solvents (in the absence of hydroxylic reagents) this is the sole route of alkyl halide decomposition. Indeed, it is not so long ago that this heterolytic pathway was established[38-40] as the major reaction route in the gas phase, where previous thought would have expected homolytic chemistry, related to dissociation along the RX covalent curve. In one widely held view,[1,6,11,13] there is in solution a common unimolecular ionization step eq 1.1 to produce an intimate ion pair for both S_N1 and E1 mechanisms. It is just this step which is the subject of this paper. In this connection, it is important to note that even in polar and nonpolar aprotic solvents, the S_N1 (nonsolvolytic) mechanism is followed if a hydroxylic reaction partner is present in sufficient concentration.[1e] In this sense, we can regard the process eq 1.1 in such solvents as a sort of limiting law S_N1 behavior, and it is in this sense that we will refer to eq 1.1 as an S_N1 ionization throughout.[41]

The outline of this paper—which focusses on the transition-state structure and free energy—is as follows. In section 2, we give an initial description of the S_N1 ionization in electron-transfer language and make connections to the original Ogg and Polanyi description. We indicate why a more general formulation is required and effect it in section 3. The theory is illustrated for a model of *t*-BuCl ionization in solvents of differing polarity in section 4. We also discuss in that section the free energetics and the location and charge distribution character of the transition state as well as their trends with solvent polarity. These aspects are analyzed from a general perspective in section 5. Concluding remarks are offered in section 6. The reaction path and nonequilibrium solvation effects on the reaction rate are examined in part 2.[26]

2. Qualitative Description of Ionic Dissociation

We will employ a simple two-state model consisting of a pure covalent state with wave function $\phi_C[RX]$ and a pure ionic state $\phi_I[R^+X^-]$ and interpret the ionic dissociation process in terms of electron-transfer processes between these two valence bond states at each RX separation coordinate value r.[42] Before we embark on this program, it is important to stress that, as we will see, this is a quite different matter than a simple assumption that there is any significant activated electron-transfer character for the reaction. This distinction is of relevance to the extensive and stimulating discussions of ionic organic reactions, invoking assorted electron-transfer ideas, by Pross,[19,20] Shaik,[19,21] and Kochi,[22] as well as in connection with the application of Marcus equations for reaction activation free energies.[43,44]

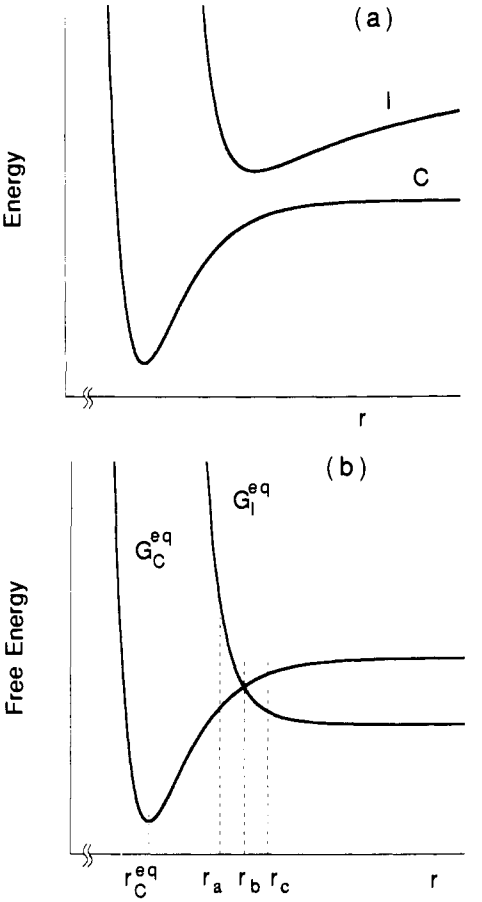

Figure 1. Schematic free energy curves for the covalent and ionic diabatic states: (a) in vacuum (the larger equilibrium separation in the ionic curve reflects the greater increase in radius for anion formation than decrease in radius for cation formation) and (b) equilibrated in a polar solvent.

The analysis in this section can be considered as a formulation (and generalization) in molecular electron-transfer terms of the Ogg–Polanyi discussion.[2] It also serves to introduce several important quantities. We will conclude that, despite its usefulness for orientation and in comprehending a number of key features of S_N1 ionization, a more fundamental analysis is necessary (section 3).

For the pure covalent state ϕ_C, the transferring electron occupies an orbital associated with R, while it occupies an X orbital for the pure electronically excited ionic state ϕ_I. The two pure diabatic states depend parametrically on the RX separation r [cf. Figure 1a]

$$\phi_C(r) = \phi_C[RX] \qquad \phi_I(r) = \phi_I[R^+X^-] \qquad (2.1)$$

(ϕ_C and ϕ_I are thus purely electronic wave functions, at fixed solute nuclear coordinates.) In this diabatic basis,[23] the vacuum Hamiltonian is represented by a 2 × 2 matrix

$$\mathcal{H}^0(r) = \begin{bmatrix} \mathcal{H}^0_{11}(r) & \mathcal{H}^0_{12}(r) \\ \mathcal{H}^0_{21}(r) & \mathcal{H}^0_{22}(r) \end{bmatrix} \qquad (2.2)$$

where $\mathcal{H}^0_{11}(r)$ and $\mathcal{H}^0_{22}(r)$ are the gas-phase diabatic potential energies associated with ϕ_C and ϕ_I, respectively [cf. Figure 1a], and $\mathcal{H}^0_{12}(r) = \mathcal{H}^0_{21}(r)$ is the vacuum electronic coupling between the two. (For a specific detailed example, see section 4A.) Note that the vacuum Hamiltonian $\mathcal{H}^0$ varies with the separation r.

In general, the two diabatic states ϕ_C and ϕ_I are not orthogonal, and their overlap integral S

$$\langle \phi_C(r) | \phi_I(r) \rangle = S(r) \qquad (2.3)$$

changes with r. It is convenient to introduce in their stead an

(38) (a) Maccoll, A.; Thomas, P. J. *Nature* **1955**, *176*, 392. (b) Maccoll, A.; Thomas, P. J. *Prog. React. Kinet.* **1967**, *4*, 119. (c) Maccoll, A. *Chem. Rev.* **1969**, *69*, 33.

(39) Benson, S. W.; Bose, A. N. *J. Chem. Phys.* **1963**, *39*, 3463. See, also: Benson, S. W.; Haugen, G. R. *J. Am. Chem. Soc.* **1965**, *87*, 4036.

(40) Rzepa, H. S. *J. Chem. Soc., Chem. Commun. (London)* **1981**, 939.

(41) While we do not here study at all the E1 process eq 1.3, our results are nonetheless directly relevant for the elimination route insofar as the ionization eq 1.1, at least to the contact ion pair stage, is in fact a common step[1] for S_N1 and E1 reactions. Even if it is not so shared[38] for these reaction classes, our present results should prove useful in assessing how it is that in nonpolar solvents the ionization step eq 1.1 could subside in importance compared to alternate less polar mechanisms[38] for unimolecular elimination.[11c]

(42) This choice obviously excludes consideration of an elimination mechanism [cf. section 1], which would require considerations of further electronic states[38,39] as well as additional nuclear coordinates.

(43) Albery, W. J.; Kreevoy, M. M. *Adv. Phys. Org. Chem.* **1978**, *16*, 87.

(44) Keeffe, J. R.; Kresge, A. J. In *Techniques of Chemistry*; Bernasconi, C. F., Ed.; Wiley: New York, 1986; Vol. 6, Part 1.

orthonormal basis $B = \{\psi_C,\psi_I\}$ defined as

$$\psi_C(r) = \phi_C(r)$$

$$\psi_I(r) = [1 - S^2(r)]^{-1/2}[\phi_I(r) - S(r)\phi_C(r)] \quad (2.4)$$

where $\psi_C(r)$ is the pure covalent state while $\psi_I(r)$ is a mixed state; the covalent character for ψ_I is approximately assessed as $\sim S^2(r)$. This square overlap is negligible unless r is very small, so $\psi_I(r)$ is mainly ionic [see also section 4A]. Thus, we will refer to $\psi_I(r)$ as an ionic state. In this orthonormal basis, the vacuum Hamiltonian becomes

$$\mathcal{H}^0(r) = \begin{bmatrix} V_C^0(r) & -\beta(r) \\ -\beta(r) & V_I^0(r) \end{bmatrix} \quad (2.5)$$

where the matrix elements in the orthonormal and diabatic bases are related by

$$V_C^0(r) = \mathcal{H}_{11}^0(r)$$

$$V_I^0(r) = [1 - S^2(r)]^{-1}[\mathcal{H}_{22}^0(r) - 2S(r)\mathcal{H}_{12}^0(r) + S^2(r)\mathcal{H}_{11}^0(r)] \quad (2.6)$$

$$-\beta(r) = [1 - S^2(r)]^{-1/2}[\mathcal{H}_{12}^0(r) - S(r)\mathcal{H}_{11}^0(r)]$$

$V_C^0(r)$ and $V_I^0(r)$ are the covalent and ionic potential energy curves in vacuum and $\beta(r)$ is the vacuum electronic coupling in the orthonormal basis.

When the solute is immersed in a polar solvent, the ionic state ψ_I will be stabilized to a certain degree with respect to the covalent state ψ_C, due to the electrostatic interactions between the solute charge distribution and the solvent polarization. The motions associated with the solvent electronic polarization $\vec{P}_{el}$ arising from the solvent electrons are usually much faster than the separation coordinate r and the solvent "orientational" polarization $\vec{P}_{or}$, which in fact involves both the (hindered and free) rotations and translations of the solvent nuclei.[30,45,46] Therefore while $\vec{P}_{el}$ always maintains its equilibrium with the solute charges and $\vec{P}_{or}$, $\vec{P}_{or}$ may not (see section 3). Thus the extent of the ionic state stabilization varies with the solvent orientational polarization. To explicitly account for this, we now introduce a collective solvent coordinate s, which gauges in an effective way the solvent orientational polarization $\vec{P}_{or}$ by

$$\vec{P}_{or} = \frac{1}{4\pi}\left(\frac{1}{\epsilon_\infty} - \frac{1}{\epsilon_0}\right)\epsilon_\infty[s\vec{\mathcal{E}}_I + (1 - s)\vec{\mathcal{E}}_C] \quad (2.7)$$

where ϵ_∞ and ϵ_0 are the optical and static dielectric constants for the solvent, and $\vec{\mathcal{E}}_I$ and $\vec{\mathcal{E}}_C$ are the vacuum electric fields arising from the solute ionic and covalent states, ψ_I and ψ_C, respectively. This represents the solvent orientational polarization in equilibrium with an effective external electric field $s\vec{\mathcal{E}}_I + (1 - s)\vec{\mathcal{E}}_C$, in the presence of the solvent electronic polarization equilibrated to the same external field. (This field need not of course be the instantaneous solute electric field, except in full equilibrium.) The electrostatic interaction ΔE between $\vec{P}_{or}$ and the difference field $\vec{\mathcal{E}}_C - \vec{\mathcal{E}}_I$ screened by the solvent electronic polarization becomes in this representation

$$\Delta E = -\frac{1}{\epsilon_\infty}\int_V d\vec{x}\vec{P}_{or}[\vec{\mathcal{E}}_C - \vec{\mathcal{E}}_I]$$

$$= s\frac{1}{4\pi}\left(\frac{1}{\epsilon_\infty} - \frac{1}{\epsilon_0}\right)\int_V d\vec{x}[\vec{\mathcal{E}}_C - \vec{\mathcal{E}}_I]^2 + \text{constant} \quad (2.8)$$

where $\vec{x}$ is a field point in the solvent, in volume V, and where the constant term is independent of the solvent coordinate s. (Vector dot products are to be understood.) In modern molecular dynamics simulation studies of charge shift reactions, the microscopic analogue of ΔE is commonly used as a solvent coordinate.[23b,47]

The pure covalent state ψ_C will be assumed to have no dipole moment, so that $\vec{\mathcal{E}}_C$ vanishes. The ionic field $\vec{\mathcal{E}}_I$ at field point $\vec{x}$ is the expectation value of the vacuum electric field operator $\vec{\mathcal{E}}_e$ taken for the ionic state ψ_I

$$\vec{\mathcal{E}}_I(\vec{x};r) = \langle\psi_I(r)|\vec{\mathcal{E}}_e(\vec{x};r)|\psi_I(r)\rangle \quad (2.9)$$

and depends on the nuclear separation r. For later use, we introduce the electrostatic energy M_s associated with the ionic field $\vec{\mathcal{E}}_I$

$$M_s(r) \equiv \frac{1}{8\pi}\int_V d\vec{x}\vec{\mathcal{E}}_I(\vec{x};r)\vec{\mathcal{E}}_I(\vec{x};r) \quad (2.10)$$

When the solvent coordinate $s = 1$, $\vec{P}_{or}$ in eq 2.7 is equilibrated to $\vec{\mathcal{E}}_I$; the solvent configuration is in equilibrium with the solute ionic state $\psi_I[R^+X^-]$. The $s = 0$ case corresponds to equilibrium with the pure covalent state. The solvent coordinate s measures the extent of the ionic state stabilization due to the solvation; the maximum stabilization occurs for $s = 1$.

For purposes of orientation, it is useful to begin the discussion by considering a diabatic $\{\psi_C,\psi_I\}$ perspective, where one would write the free energy curves for the two states as[48]

$$G_C(r,s) = V_C^0(r) + \Delta G_r(r)s^2 = G_C^{eq}(r) + \Delta G_r(r)s^2$$

$$G_I(r,s) = V_I^0(r) - \Delta G_r^{el}(r) - 2\Delta G_r(r)s + \Delta G_r(r)s^2 \quad (2.11)$$

$$= G_I^{eq}(r) + \Delta G(r)(1 - s)^2$$

where the r-dependent equilibrium free energy[49] for the ionic state is [Figure 1b]

$$G_I^{eq}(r) = G_I(r,s = 1) = V_I^0(r) - \Delta G_r^{el}(r) - \Delta G_r(r)$$

$$= V_I^0(r) + \Delta G_{I,solv}^{eq}(r) \quad (2.12)$$

Here $\Delta G_r(r)$ is the solvent reorganization energy [Figure 2a]

$$\Delta G_r(r) = G_I(r,s = 0) - G_I(r,s = 1) = \left(\frac{1}{\epsilon_\infty} - \frac{1}{\epsilon_0}\right)M_s(r) \quad (2.13)$$

measuring the ultimate free energy change subsequent to a Franck–Condon transition $\psi_C \rightarrow \psi_I$ at a given r and associated with the orientational polarization. (Note that via eq 2.8, $\Delta G_r(r)$ is related to the electrostatic interaction between $\vec{P}_{or}$ and $\vec{\mathcal{E}}_I$.) In an analogous fashion, we have defined

$$\Delta G_r^{el}(r) = \left(1 - \frac{1}{\epsilon_\infty}\right)M_s(r) \quad (2.14)$$

as the negative of the equilibrium free energy of solvation of the ionic state by the solvent electronic polarization. $\Delta G_r^{el}(r)$ could also be regarded as a reorganization energy, associated with the

(45) Marcus, R. A. *J. Chem. Phys.* **1956**, *24*, 966, 979. *Faraday Discuss. Chem. Soc.* **1960**, *29*, 21. *J. Chem. Phys.* **1963**, *38*, 1858. *Annu. Rev. Phys. Chem.* **1964**, *15*, 155.

(46) For some general reviews, see: Sutin, N. *Prog. Inorg. Chem.* **1983**, *30*, 441. Newton, M. D.; Sutin, N. *Annu. Rev. Phys. Chem.* **1984**, *35*, 437. Marcus, R. A.; Sutin, N. *Biochim. Biophys. Acta* **1985**, *811*, 265.

(47) (a) Warshel, A.; Hwang, J. K. *J. Chem. Phys.* **1986**, *84*, 4938. (b) Halley, J. W.; Hautman, J. *Phys. Rev. B* **1988**, *38*, 11704. (c) Kuharski, R. A.; Bader, J. S.; Chandler, D.; Sprik, M.; Klein, M.; Impey, R. W. *J. Chem. Phys.* **1988**, *89*, 3248. (d) Carter, E. A.; Hynes, J. T. *J. Phys. Chem.* **1989**, *93*, 2184. (e) Zichi, D. A.; Ciccotti, G.; Hynes, J. T.; Ferrario, M. *J. Phys. Chem.* **1989**, *93*, 6261. (f) Borgis, D.; Hynes, J. T. *J. Chem. Phys.* **1991**, *94*, 3619. (g) Fonseca, T.; Ladanyi, B. M. *J. Phys. Chem.* **1991**, *95*, 2116. (h) Carter, E. A.; Hynes, J. T. *J. Chem. Phys.* **1991**, *94*, 5961.

(48) If the internal degrees of freedom of RX were accounted for, the vacuum potentials V_C^0, V_I^0 would themselves be replaced by temperature dependent free energies.

(49) Free energies which appear in eq 2.11 are quasi-free energies in which one (or more) coordinate(s) has been removed. They are not coordinate-independent full free energies, and one should properly always refer to them as surfaces or curves. In the interest of economy of presentation, however, we will often drop this precision where there is no danger of confusion. In addition, a rotational contribution [cf. eq 3.2] is ignored in this section for simplicity.

solvent electronic polarization in a purely hypothetical situation where the $\vec{P}_{el}$ motion is slow. Note that $\Delta G_r^{el}(r)$ and $\Delta G_r(r)$ are, respectively, also the self-energies associated with $\vec{P}_{el}$ and $\vec{P}_{or}$, both induced by the ionic field $\vec{\mathcal{E}}_I$ [cf. eq 2.9]. Their sum is the negative of the equilibrium solvation free energy $\Delta G_{I,solv}^{eq}$ of the ionic state.[30a] Equation 2.11 shows that $2\Delta G_r(r)$ is the force constant

$$K_s^0(r) = 2\Delta G_r(r) \tag{2.15}$$

gauging the ease of solvent orientational polarization fluctuations in the presence of either the ψ_C or ψ_I solute state at a given RX separation r. Finally, any cavity potential effects of the solvent are neglected compared to electrostatic interactions (see ref 84 below).[50]

If one simply couples these two curves G_C and G_I via the electronic coupling β—as is conventional in electron-transfer theory,[46] the resulting electronically adiabatic free energy curves are

$$G_\pm = \frac{G_I + G_C}{2} \pm \frac{1}{2}\sqrt{(\Delta G)^2 + 4\beta^2} \tag{2.16}$$

where the free energy difference $\Delta G(r) \equiv G_I(r) - G_C(r)$. In particular, the lowest adiabatic curve is

$$G_- = G_C + \frac{\Delta G}{2} - \frac{1}{2}\sqrt{(\Delta G)^2 + 4\beta^2} \tag{2.17}$$

with the ionic-covalent state gap given by

$$\Delta G(r,s) = \Delta G_{eq}(r) + 2\Delta G_r(r)\left(\frac{1}{2} - s\right)$$

$$\Delta G_{eq}(r) = G_I^{eq}(r) - G_C^{eq}(r) \tag{2.18}$$

The solvent-equilibrated uncoupled diabatic curves $G_{C,I}^{eq}$ sketched in Figure 1b is a schematic valence bond correlation diagram.[19] Near the covalent well at small r, the lower diabatic state is covalent while its counterpart with product state electronic structure (i.e., ionic state) is much higher in energy. For large RX separation, the situation is reversed: the ionic state is lower in energy owing to the solvent stabilization. The ionic curve decreases monotonically in this region due to a better solvation progressively with r and to a decreasing short-range repulsion, while the covalent curve is monotonically increasing due to the bond rupture. In the language of Pross and Shaik,[19] the crossing (or avoided crossing) takes place between the two valence bond states—here the solvent equilibrated diabatic states—with the reactant and product electronic structure (i.e., the covalent and ionic states); as a result, a barrier is formed for both forward and reverse processes.

The uncoupled diabatic curves in the solvent coordinate are sketched in Figure 2 for the three different separations r indicated in Figure 1b. Also shown there are the adiabatic curves $G_\pm(r)$ eq 2.16 for a modest amount of electronic coupling. In proceeding to larger r, the base G_C^{eq} rises as the covalent bond is stretched, while the base G_I^{eq} falls due to the more favorable solvation, for the two solvent wells. Case b is of particular interest: it corresponds to the crossing of the equilibrated curves in Figure 1b. An initial guess at the transition state suggested by Figure 1b, and seemingly implied by Ogg and Polanyi in their pioneering study,[2] is just this point: $r = r_{cr} = r_{eq}^\ddagger$ such that $G_C^{eq} = G_I^{eq}$. But this requires closer scrutiny. Equation 2.17 tells us that the activation free energy with this choice would have to satisfy

$$\Delta G^\ddagger = G_-^\ddagger - G_C^{eq}(r_C^{eq})$$

$$= G_C(r_{eq}^\ddagger) + \Delta G_r\left(\frac{1}{2} - s\right) - \frac{1}{2}\sqrt{\Delta G_r^2(1-2s)^2 + 4\beta^2} - G_C^{eq}(r_C^{eq}) \tag{2.19}$$

where r_C^{eq} locates the covalent reactant potential minimum, since from eq 2.18 and $\Delta G_{eq} = 0$, here $\Delta G = \Delta G_r(1-2s)$. (Note that the s value to be used here is so far ambiguous, since in Figure 1b for the equilibrated covalent state $s = s_{eq} = 0$ and for the equilibrated ionic state, $s = s_{eq} \approx 1$.) But Figure 2b shows that, with only modest electronic coupling such that $\beta < \Delta G_r/4$, there would *still* be an activation barrier to cross in the solvent coordinate not apparent in Figure 1b, i.e., an activated electron-transfer reaction. There is thus an inconsistency, since the lowest *net* barrier in both r and s would lie at some other r than this $r^\ddagger$ choice.

However, when the electronic coupling is sufficiently strong, namely $\beta > \Delta G_r/4$, Figure 2 is not at all the correct picture. As shown in Figure 3, such a potent coupling at $r_{eq}^\ddagger$ will completely obliterate the solvent barrier, leaving instead two solvent *wells*. In particular, the lower well, associated at $r = r_{eq}^\ddagger$ with the symmetric *delocalized* wave function

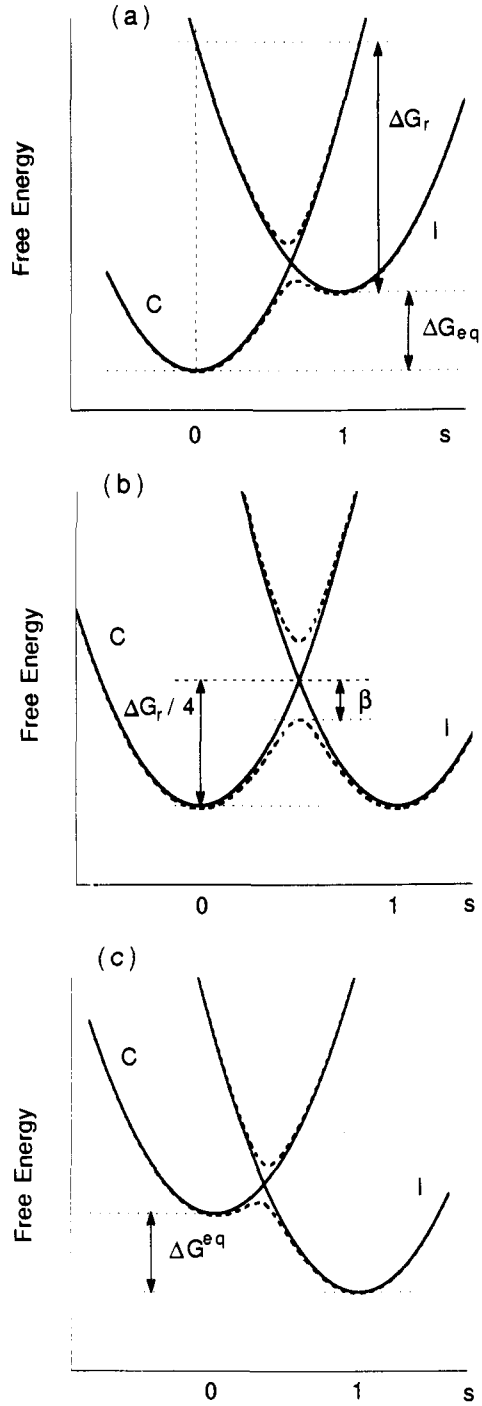

Figure 2. Schematic free energy curves along the solvent coordinate s at fixed RX separation r in solution: (a) $r = r_a$, (b) $r = r_b$, and (c) $r = r_c$. The electronic coupling β is small compared to ΔG_r. The lower and upper dashed lines denote $G_-(r)$ and $G_+(r)$, respectively.

(50) Entelis, S. G.; Tiger, R. P. *Reaction Kinetics in the Liquid Phase*; Wiley: New York, 1976.

$$\Psi_S = \frac{1}{\sqrt{2}}(\psi_C + \psi_I) \tag{2.20}$$

has its minimum located, by symmetry, at $s = 1/2$,[51] and eq 2.19 becomes

$$\Delta G^{\ddagger} = G_C^{eq}(r_{eq}^{\ddagger}) - G_C^{eq}(r_C^{eq}) - \beta + \Delta G_r/4$$
$$= \Delta G_{cr}^{\ddagger} - \beta + \Delta G_r/4 \tag{2.21}$$

where $\Delta G_{cr}^{\ddagger}$ is the free energy difference between the crossing point and the reactant state. This states that the activation free energy is composed of (a) the free energy cost $\Delta G_{cr}^{\ddagger}$ to stretch the bond in the covalent state to the point where $G_C^{eq} = G_I^{eq}$, (b) the cost $\Delta G_r/4$ to reorganize the solvent to be appropriately in equilibrium, and (c) an electronic coupling contribution. Notice that there is *no* activated electron transfer involved at $r = r_{cr} = r_{eq}^{\ddagger}$.

Though not stated in these terms by Ogg and Polanyi, it seems fair to say that our description above is the modern, electron-transfer perspective which formalizes (and extends) some aspects of their discussion. But compared to the description by these authors which would give $\Delta G_{cr}^{\ddagger} - \beta$ for the activation free energy $\Delta G^{\ddagger}$, there is a significant, additional solvent reorganization energy $\Delta G_r/4$ contribution. The source of this contribution is clearly traceable in eq 2.21 and Figures 2b and 3b. It is not at all an insignificant component of $\Delta G^{\ddagger}$: for example, we estimate in section 4B that $\Delta G_r/4$ is about 3~4 kcal/mol for *t*-BuCl in highly polar solvents. While the appearance of $\Delta G_r/4$ in the S_N1 arena is novel, it is no surprise from an electron-transfer[45,46] perspective. Nonetheless, eq 2.21 is not satisfactory, as we now discuss.

3. Theoretical Formulation

While the analysis in section 2 is a useful guide, it suffers from several serious defects. First, the equilibrium location of the solvent at the putative transition-state location $r_{eq}^{\ddagger}$ is $s_{eq} = 1/2$, which with eq 2.7 says that the transition-state charge distribution is always 50% ionic. This is in our view decidedly difficult to accept as valid for all ionizations and all solvents; clearly additional factors must be taken into account.[52] Second, the standard electron-transfer diagonalization procedure is in fact incorrect for moderate to large electronic coupling[30]—which as we will see, is the applicable coupling regime for typical S_N1 ionizations. In the present context, the difficulty is the following. In eq 2.11 the electronic polarization is equilibrated to the two diabatic states—in our case only contributing for ψ_I—and then the coupling mixes the two states. But this is actually generally incorrect; it keeps the electronic polarization equilibrated to the localized wave function ψ_I even in the presence of the coupling. Whereas in fact, the lowest free energy electronic wave function at $r_{eq}^{\ddagger}$ is the symmetric state Ψ_S eq 2.20, and one might expect that the electronic polarization should actually be equilibrated to the delocalized charge distribution associated with Ψ_S^2—as is, in effect, the common practice in models[50,53,54] of transition state solvation—or to a charge distribution between these two extremes. The diagonalization procedure fails to allow the electronic polarization to readjust to the evolving electronic charge distribution.[30] This failure can have an impact on the solvent contribution to the activation free energy. To surmount these difficulties, we turn now to a more fundamental approach to the electronic structure–solvent coupling problem for S_N1 ionizations.

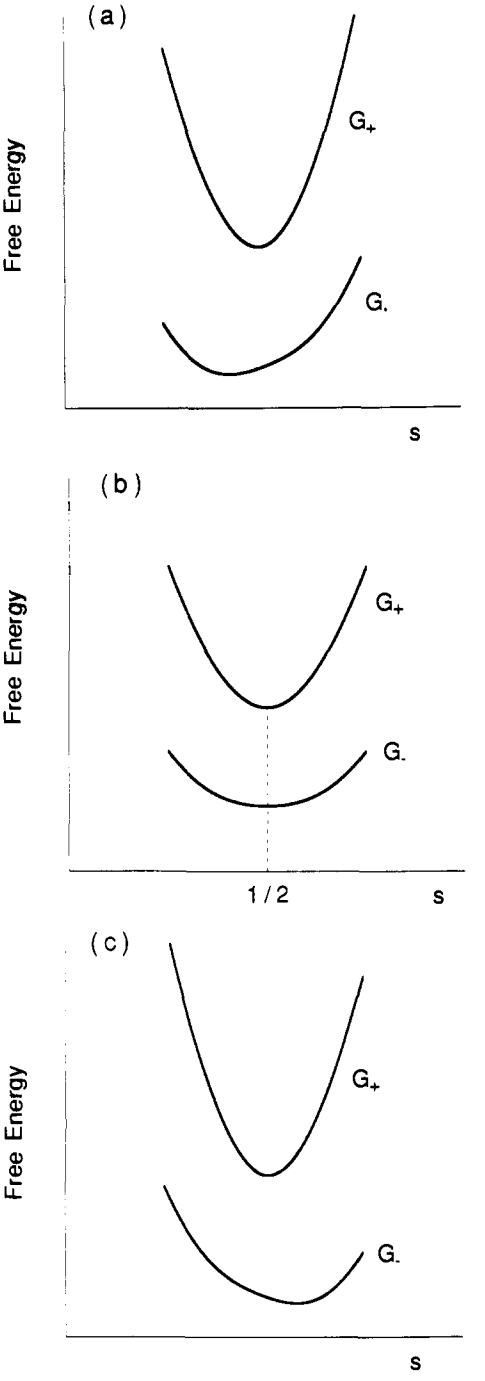

Figure 3. Schematic free energy curves along s in the strong electronic coupling limit. (a) $r = r_a$ and (b) $r = r_b$, and (c) $r = r_c$. The coupling is large enough to overcome the localizing tendency of the solvent polarization and leave a single stable well for each adiabatic free energy surface.

To this end, we will employ our nonlinear Schrödinger equation formulation for electron-transfer processes,[27] generalized to S_N1 ionic dissociation reactions. The generalization is reasonably straightforward from a formal viewpoint, since the single additional feature for S_N1 ionizations compared to electron-transfer processes is the (extremely important) r-dependence in the two-state basis functions and vacuum Hamiltonian, here ψ_C, ψ_I, and $\mathcal{H}^0$. This introduces an essential extra coordinate in describing S_N1 reactions. In what follows, a Born–Oppenheimer approximation (for solvent and solute *nuclear* degrees of freedom) is made, in that the electronic energy arising from both the solute and solvent electronic wave functions is found as a function of the solute and solvent nuclear coordinates. The goal is to obtain the free energies, eqs 3.11 and 3.14 below, correctly describing the S_N1 system both when the solvent is not or is in equilibrium. Note also that the

(51) The electric field arising from the symmetric delocalized state Ψ_S is the expectation value $\bar{\mathcal{E}}_S = \langle\Psi_S|\hat{\mathcal{E}}_e|\Psi_S\rangle$. Under the assumption that $\bar{\mathcal{E}}_I = \langle\psi_I|\hat{\mathcal{E}}|\psi_I\rangle$ is the only nonvanishing element for $\bar{\mathcal{E}}_e$, we obtain $\bar{\mathcal{E}}_S = \bar{\mathcal{E}}_I/2$. In view of eq 2.7, the s value associated with the solvent orientational polarization in equilibrium with $\bar{\mathcal{E}}_S = \bar{\mathcal{E}}_I/2$ is $^1/_2$.

(52) Even a full analysis of eq 2.19 would indicate that, due to the electronic coupling and asymmetry of the diabatic curves,[9b,21a] the barrier is not located at the crossing point of the equilibrated diabatic curves and the transition-state wave function is not 50% ionic. We omit this analysis because it suffers from the error regarding the electronic polarization described in the text. We will, however, return to these issues in section 5.

(53) Laidler, K. J. *Chemical Kinetics*, 3rd ed.; Harper and Row: New York, 1987.

(54) Marcus, R. A. *Faraday Symp. Chem. Soc.* **1975**, *10*, 60.

solute electronic structure is solvent-dependent at any r in (and out of) equilibrium. This solute "polarizability" effect[27,30b,55] would be absent in various prescriptions based on solvating gas-phase electronically adiabatic structures.[56]

3.A. Nonequilibrium Free Energy. We begin by summarizing the relevant results of ref 27 (to which the reader is referred for a detailed discussion) and extending them to include r-dependence in the solute wave function. The general free energy expression for the quantum two-state solute + solvent system in the presence of arbitrary solvent orientational polarization $\vec{P}_{or}$ and equilibrated solvent electronic polarization $\vec{P}_{el}$ can be formally written as a weighted sum[27]

$$G[\Psi,\vec{P}_{or}] = (1-f)G_{BO}[\Psi,\vec{P}_{or}] + fG_{SC}[\Psi,\vec{P}_{or}]$$

$$f \equiv \frac{\rho}{2c_C c_I + \rho} \tag{3.1}$$

where G_{BO} and G_{SC} are the free energies in the Born–Oppenheimer (BO) and self-consistent (SC) approximations (described below) for $\vec{P}_{el}$, respectively

$$G_{BO,SC} = \langle\Psi|\mathcal{H}^0|\Psi\rangle - k_B T \ln [r/r_0]^2 - \frac{1}{8\pi}\left(1-\frac{1}{\epsilon_\infty}\right)\int_V d\vec{x} A_{BO,SC} - \frac{1}{\epsilon_\infty}\int_V d\vec{x}\,\langle\Psi|\vec{\mathcal{E}}_e|\Psi\rangle\vec{P}_{or} + \frac{2\pi\epsilon_0}{\epsilon_\infty(\epsilon_0-\epsilon_\infty)}\int_V d\vec{x}\vec{P}_{or}\vec{P}_{or} \tag{3.2}$$

$$A_{BO} = \langle\Psi|\vec{\mathcal{E}}_e^2|\Psi\rangle \qquad A_{SC} = \langle\Psi|\vec{\mathcal{E}}_e|\Psi\rangle^2$$

(The ln $[r/r_0]^2$ term here arises from the thermal average over the solute rotational degrees of freedom;[57] since what matters is the relative free energy; we have introduced a reference distance r_0, set to be the equilibrium bond length for convenience.) Here Ψ is an arbitrary solute state described as a linear combination of the covalent and ionic states

$$\Psi(r,s) = c_C(r,s)\psi_C(r) + c_I(r,s)\psi_I(r) \tag{3.3}$$

in the orthonormal two-state basis $\{\psi_C,\psi_I\}$, and $\vec{\mathcal{E}}_e$ is the solute electric field operator in vacuum. ρ in eq 3.1 is a dimensionless parameter

$$\rho \equiv 2\beta/\hbar\omega_{el} \tag{3.4}$$

where $\hbar$ is Planck's constant divided by 2π, ω_{el} is the frequency associated with the solvent electronic polarization $\vec{P}_{el}$, and β is the solute electronic coupling in eq 2.5. As shown in ref 27, the time scale associated with the $\vec{P}_{el}$ rearrangement is governed by its frequency ω_{el}, while that associated with the solute charge shift is proportional to the electronic coupling between the two diabatic states; thus ρ is an important parameter gauging the two time scales. In fact, the factor in eq 3.1 is[27]

$$f = (\tau_{el} + \tau_{tr})^{-1}\tau_{el} \tag{3.5}$$

and explicitly depends on the time scales $\tau_{el} = 2\pi/\omega_{el}$ for $\vec{P}_{el}$ and $\tau_{tr} = 2\pi\hbar c_I c_C/\beta$ for the transferring solute electron.

The BO limit for the electronic polarization is attained when $\vec{P}_{el}$ is much faster than the solute electron shift (i.e., $\rho \to 0, f \to 0$).[27] In this scheme, $\vec{P}_{el}$ completely solvates the solute whatever the solute electronic state may be. There is no free energy change due to $\vec{P}_{el}$ whether the solute is charge-localized or charge-delocalized.[27,31] In the opposite limit $\rho \to \infty, f \to 1$, and $\vec{P}_{el}$ much slower than the solute electron shift, the SC scheme is proper for the electronic polarization. $\vec{P}_{el}$ becomes equilibrated to the solute charge distribution determined by $|\Psi|^2$. In this limit, a charge delocalized solute state is disfavored by $\vec{P}_{el}$ over a charge localized state.[27]

The typical $\vec{P}_{el}$ time scale ranges[27] from 0.03 ($\hbar\omega_{el} \sim 20$ eV) to 0.3 fs ($\hbar\omega_{el} \sim 2$ eV). The solute charge shift time can vary by several orders of magnitude depending on β; our strongly coupled S_N1 solute is characterized by a time scale ~0.5 fs, i.e., $\beta \approx 15$ kcal/mol (see sections 4A and 5B). For the solute + solvent systems studied here ($\hbar\omega_{el} \approx 4$ eV[58]), $\vec{P}_{el}$ can be treated neither in the BO nor the SC approximation. We thus need a proper quantum $\vec{P}_{el}$ description that takes into account the relative time scales,[27] discussed in ref 27, and properly incorporated in eq 3.1. This quantum description provides a significant improvement over the BO[31,32] and self-consistent[30,54,59] treatments for $\vec{P}_{el}$ and their equilibrium analogues,[28,29] which are commonly employed for a wide variety of charge shift and transfer problems and electronic structure calculations in solution.

By invoking the variational principle[60] that the actual solute wave function is the one which minimizes the free energy, i.e., $\delta G/\delta\Psi(r) = 0$, we can obtain the Schrödinger equation for Ψ

$$\mathcal{H}[\Psi, \vec{P}_{or}]\Psi = E\Psi \tag{3.6}$$

whose explicit form, which we do not require here, is given in ref 27. The energy eigenvalue is E. This equation is, in general, nonlinear in Ψ due to the electrostatic interaction between the solute and the equilibrated $\vec{P}_{el}$, which depends upon Ψ. By solving it [cf. section 3B], we can determine the solute wave function Ψ in terms of the solvent orientational polarization $\vec{P}_{or}$ (and the RX separation r)—the solute electronic structure varies with the fluctuating $\vec{P}_{or}$. Since $\vec{P}_{or}$ is arbitrary, the wave function $\Psi[\vec{P}_{or}]$ thus obtained describes, in general, a *nonequilibrium solvation* state for the solute molecule at each value of r. This $\vec{P}_{or}$- and r-dependent wave function will be called the nonequilibrium solvation stationary state. When $\Psi[\vec{P}_{or}]$ is substituted into eq 3.1, G is obtained in terms of $\vec{P}_{or}$ and r. This G defines the reaction free energy surface, on which an ionic dissociation process RX $\to R^+X^-$ takes place.

3.B. Formal Solution. We now proceed to formally solve the nonlinear Schrödinger equation and obtain the reaction free energy surface. In a polar solvent, the state coefficients c_C,c_I depend not only on the RX separation r but also on the fluctuating orientational polarization $\vec{P}_{or}$ and thus on the solvent coordinate s, eq 2.7. We can determine these coefficients by substituting eqs 2.7 and 3.3 into the nonlinear Schrödinger eq 3.6. In order to proceed along this route, we first need the matrix elements for the electric field $\vec{\mathcal{E}}_e$. In view of eq 2.4, $\vec{\mathcal{E}}_I$ is given by[61]

$$\vec{\mathcal{E}}_I(\vec{x};r) = [1 - S^2(r)]^{-1}\vec{\mathcal{E}}_I^0(\vec{x};r) \tag{3.7}$$

where $\vec{\mathcal{E}}_I^0(\vec{x};r)$ is the electric field at point $\vec{x}$ arising from the pure ionic state $\phi_I(r)$,[62] i.e., the carbocation R^+ and the negative ion X^- at a fixed separation r

(55) Juanós i Timoneda, J.; Hynes, J. T. *J. Phys. Chem.* **1991**, *95*, 10431.

(56) See, e.g.: Tucker, S. C.; Truhlar, D. G. *J. Am. Chem. Soc.* **1990**, *112*, 3347.

(57) Sceats, M. *Adv. Chem. Phys.* **1988**, *70*, 357. We neglect, for simplicity, rotational dielectric friction,[35] whose net effect on the energetics of *t*-BuCl should be small due to the large moment of inertia.

(58) This is approximately a UV absorption energy [Grasselli, J. G.; Ritchey, W. M. *Atlas of Spectral Data and Physical Constants for Organic Compounds*; CRC: Cleveland, 1975] for the three solvents studied here.

(59) For solvated electron energy level calculations in the self-consistent and Born–Oppenheimer approximations, see: Jortner, J. *Mol. Phys.* **1962**, *5*, 257.

(60) See, for example: Karplus, M.; Porter, R. N. *Atoms and Molecules*; Benjamin: Reading, 1970.

(61) Recall that the covalent state is assumed to have no dipole moment. The other matrix elements could also be included if desired. See: Kim, H. J.; Hynes, J. T. *Solute Electronic Structure and Solvation in Time-Dependent Fluorescence: I. Formulation and Application to a Two-State Model*; To be submitted for publication. In general, the electronic coupling becomes renormalized due to the off-diagonal element (i.e., exchange field) of the electric field operator.[27,30] However, the renormalization effect is rather small[30b] (≲15% for a contact pair with a separation of 3.7 Å with $S^2 \approx 0.1$); the effect will become even smaller for the tighter RX complexes considered here because the solvent reorganization free energy is smaller. We thus neglect the exchange field completely here for simplicity.

(62) It may seem somewhat perplexing that the electric field $\vec{\mathcal{E}}_I$ is stronger than $\vec{\mathcal{E}}_I^0$ in eq 3.7. This feature is due to the fact that by mixing the two pure states $\phi_{C,I}$, the ionic state ψ_I becomes more polar. In the simplest terms, we can regard the solute molecule as $2e^- + R^+ + X^+$. In the pure state ϕ_C, the two electrons occupy a covalent bonding orbital so that the electron density is large in the region between R^+ and X^+. The pure ionic state ϕ_I corresponds to the two electrons occupying an X orbital. The electron density is the same in the region between R^+ and X^+ and beyond X^+ when viewed from R^+ in this pure ionic state. Now the two states mix according to eq 2.4, the electron density decreases between R^+ and X^+ and slightly increases beyond X^+. After proper wave function normalization, this results in more electron density further out from X and R, yielding a net dipole moment pointing from X to R, responsible for the $\vec{\epsilon}_I$ strength enhancement.

$$\vec{\mathcal{E}}_I^0(\vec{x};r) = \langle\phi_I(r)|\vec{\mathcal{E}}_e(\vec{x};r)|\phi_I(r)\rangle \tag{3.8}$$

With these relations, we can obtain an algebraic equation for the $\{c_i\}$ from the nonlinear Schrödinger eq 3.6

$$\beta(c_C^2 - c_I^2) - \Delta V c_C c_I = \Delta G_r^{el}\frac{f(1+f)}{2}c_C c_I(c_C^2 - c_I^2)$$

$$c_C^2 + c_I^2 = 1 \tag{3.9}$$

which we will use to determine $\{c_i\}$. Here ΔV is the free energy difference between the covalent and ionic states in the solvent in the absence of the coupling [cf. eq 2.11]

$$\Delta V(r,s) \equiv V_I(r,s) - V_C^0(r)$$

$$V_I(r,s) \equiv V_I^0(r) - \Delta G_r^{el}(r) - 2\Delta G_r(r)s \tag{3.10}$$

$$= V_I^0(r) + \Delta G_{I,solv}^{eq}(r) + \Delta G_r(r)(1-2s)$$

V_I is the ionic potential in the absence of the coupling β, stabilized in the solvent configuration described by the solvent coordinate s, i.e., G_I in eq 2.11 minus the self-energy $\Delta G_r s^2$ associated with the orientational polarization. The free energies ΔG_r^{el} and ΔG_r are the reorganization energies associated with the solvent electronic and orientational polarizations induced by $\vec{\mathcal{E}}_I$ [eqs 2.13 and 2.14]. They measure the solvent stabilization due to the distinct solvent polarizations. In particular, the free energy for the ionic state is considerably lowered compared to the pure covalent state due to *both* ΔG_r^{el} and ΔG_r in eq 3.10. The free energy can be written in terms of the state coefficients as

$$G(r,s) = V_C^0(r)c_C^2 + V_I(r,s)c_I^2 - 2\beta(r)c_C c_I + \Delta G_r^{el}(r)\,[1-c_I^2]c_I^2 f + \Delta G_r(r)s^2 - k_B T \ln\,[r/r_0]^2 \tag{3.11}$$

which we will use for numerical evaluation of the nonequilibrium free energy. The fifth term on the right-hand side of eq 3.11 is the self-energy associated with the solvent orientational polarization,[30a,d] while the fourth term is the delocalization free energy cost associated with $\vec{P}_{el}$.[27] The latter is quartic in the state coefficient c_I because of the general nonlinear aspect that $\vec{P}_{el}$ depends on the solute electronic configuration. The degree of this dependence is governed by the factor f, eq 3.5, comparing the solute and solvent electronic time scales. It vanishes in the (BO) treatment of section 2.

The very important, albeit special, situation of equilibrium solvation occurs when $\vec{P}_{or}$ as well as $\vec{P}_{el}$ is in equilibrium with the solute charge distribution, so that

$$\frac{\partial G}{\partial s} = 0 \tag{3.12}$$

the solvent orientational polarization adjusts completely to the solute reaction system so that the free energy is a minimum along the solvent coordinate s for any fixed r. This will define, in general, a curve on an (r, s) surface; along this curve, there is *maximum* solvation, because both solvent polarizations are in equilibrium with the solute. We will call this the *equilibrium solvation path* (ESP).[17,18,30d,35] It is easy to verify from eqs 3.9, 3.11, and 3.12 that equilibrium solvation holds when

$$s = s_{eq} = c_I^2 \tag{3.13}$$

i.e., the solvent coordinate equals the actual ionic state occupation probability at a given r. The state coefficients satisfying this full equilibrium relation eq 3.12, or equivalently eq 3.13, can be determined by the equilibrium reaction potential (or reaction field) method as shown in refs 27 and 30a. Solving eq 3.9 under the equilibrium condition eq 3.12 is nontrivial since the state coefficients are functions of s, i.e., the solute charge distribution varies along the equilibrium solvation path. The solutions for the state coefficients $\{c_C^{eq}, c_I^{eq}\}$ and the solvent coordinate s_{eq} define the equilibrium solvation states, where both the solvent electronic and orientational polarizations are in full equilibrium with the solute charges.[27] (Explicit examples of the ESP will be given in section 4 and part 2.) Along the ESP, eq 3.11 reduces, with eq 3.13, to the simpler form

$$G_{eq} = V_C^0 c_C^{eq2} + V_I^0 c_I^{eq2} - k_B T \ln\,[r/r_0]^2 - 2\beta c_C^{eq}c_I^{eq} + \Delta G_{solv}^{eq} \tag{3.14}$$

i.e., the weighted average of the vacuum potentials, minus a coupling term, and the equilibrium solvation free energy

$$\Delta G_{solv}^{eq} = (1-f^{eq})\Delta G_{solv,BO}^{eq} + f^{eq}\Delta G_{solv,SC}^{eq}$$

$$f^{eq} = \frac{\rho}{2c_C^{eq}c_I^{eq} + \rho}$$

$$\Delta G_{solv,BO}^{eq} = -\Delta G_r^{el}c_I^{eq2} - \Delta G_r c_I^{eq4} = -\left(1 - \frac{1}{\epsilon_\infty}\right)M_s c_I^{eq2} - \left(\frac{1}{\epsilon_\infty} - \frac{1}{\epsilon_0}\right)M_s c_I^{eq4}$$

$$\Delta G_{solv,SC}^{eq} = -[\Delta G_r^{el} + \Delta G_r]c_I^{eq4} = -\left(1 - \frac{1}{\epsilon_0}\right)M_s c_I^{eq4} \tag{3.15}$$

referenced to the vacuum value with the same electronic structure (c_C^{eq}, c_I^{eq}). Here $\Delta G_{solv,BO}^{eq}$ and $\Delta G_{solv,SC}^{eq}$ are the solvation free energies in the Born–Oppenheimer and self-consistent field approximations.[27] The first member in eq 3.15 can be regarded as a generalization of the Born formula,[30a] as can be BO and SC solvation free energies.[27] ΔG_{solv}^{eq} allows for the proper solvation of the mixed solute charge distribution by $\vec{P}_{el}$. In contrast, the treatment of section 2 is in the BO approximation. Application of eqs 3.14 and 3.15 to find the analogue of the activation free energy eq 2.21 gives an extra contribution $f\Delta G_r^{el}/4$ compared to that result. This extra contribution is maximal at $f = 1$, when ΔG_{solv}^{eq} would be equivalent to the result of an SC treatment[30,54] and some traditional treatments.[50,53] Equation 3.14 will be used in section 5 to analyze the activation free energy.

By solving eq 3.9, we can determine the state coefficients $\{c_i\}$. Since $\vec{P}_{or}$ is in general arbitrary (and therefore so is s), these solutions describe the solute electronic structure for arbitrary conditions of nonequilibrium solvation, i.e., where the solvent electronic polarization is in equilibrium with the solute charge distribution but the solvent orientational polarization may not be. It is only when $\vec{P}_{or}$ is in equilibrium with the solute charge distribution as in eq 3.13, that there is full equilibrium solvation for fixed RX separation r.

The solution of the nonlinear eq 3.9 and construction of the free energy profile on the two-dimensional (r,s)-surface via eq 3.11 determines the S_N1 ionization free energy surface as a function of the solvent coordinate s and the internuclear separation r. In this paper and the following paper in this issue,[26] we effect the solution via an accurate perturbation method,[63] starting from the $\rho = 0$ case; this method is discussed in detail in ref 27. We now use this method to explicitly calculate the reaction free energy surface for the S_N1 ionic dissociation for a model of *tert*-butyl chloride in solution.

4. Model Calculations for *t*-BuCl in Several Solvents

In this section we use our theory to analyze the ionic dissociation of *t*-BuCl in solution by adopting a specific implementation of the two-state model introduced in section 2. We begin by specifying the vacuum Hamiltonian $\mathcal{H}^0(r)$.

4.A. Vacuum Hamiltonian. We consider first the pure ionic state. The pure ionic state potential $\mathcal{H}_{22}^0(r)$ in vacuum consists of long-range electrostatic interactions and short-range repulsive interactions. We use here a model potential designed by Jorgensen et al. for a *tert*-butyl carbocation and a chloride ion.[64] The *tert*-butyl cation is assumed to be composed of a central carbon

(63) The perturbation expansion in ΔG_r^{el} is rather accurate for the (r,s) region relevant to the S_N1 ionization, compared to the exact results obtained by solving eq 3.9 numerically. This has been checked by comparing the two results for a few sample points. In addition, we have solved the nonlinear Schrödinger equation by a nonperturbative basis set method [Kim, H. J.; Bianco, R.; Gertner, B. J.; Hynes, J. T. *J. Phys. Chem.*, in press]; the results agree with those presented here and in part 2 to better than 1%.

(64) Jorgensen, W. L.; Buckner, J. K.; Huston, S. E.; Rossky, P. J. *J. Am. Chem. Soc.* **1987**, *109*, 1891.

Table I. Parameters

$E_g(r)$

D (kcal/mol)	r_g (Å)	$k = 2a^2D$ (mdyne/Å)	a (Å^{-1})
81.2	1.803	2.8	1.583

$H^0_{11}(r)$

D_0 (kcal/mol)	$r_0(=r_g)$ (Å)	$2a_0^2D_0(=2a^2D)$ (mdyne/Å)	a_0 (Å^{-1})
66	1.803	2.8	1.757

$H^0_{22}(r)$

a_1 (kcal/mol)	a_2 (kcal/mol)	b_1 (Å)	b_2 (Å)	l (Å)	IP (kcal/mol)	EA (kcal/mol)
0.307	0.435	3.152	3.640	1.475	164.4	82.8

atom and three methyl groups in a planar geometry with C_3 symmetry about the molecular axis passing through the central carbon atom; the carbon–methyl bond length l employed is 1.475 Å. Each of the three methyl groups is positively charged with +0.2e while the central carbon has a partial charge +0.4e. This ionic state planar geometry is assumed to be maintained during the ionization process. (Thus the *t*-Bu moiety hybridization change is not dynamically accounted for. However, presumably its associated energetics are to some degree taken into account via the use of experimental energetic information in constructing the covalent and ionic potential curves.) The chloride ion is restricted to move on the C_3 symmetry axis of the *tert*-butyl ion, and the interactions with each *tert*-butyl cation constituent are modeled by a short-range Lennard-Jones potential plus a long-range Coulombic interaction

$$\mathcal{H}^0_{22}(r) = a_1\left[\left(\frac{b_1}{r}\right)^{12} - \left(\frac{b_1}{r}\right)^{6}\right] - \frac{0.4e^2}{r} + 3a_2\left[\left(\frac{b_2^2}{r^2+l^2}\right)^{6} - \left(\frac{b_2^2}{r^2+l^2}\right)^{3}\right] - \frac{0.6e^2}{\sqrt{r^2+l^2}} + \Delta \quad (4.1)$$

Here r is the distance between the central carbon atom and the chloride ion and the ionization potential for the *tert*-butyl radical minus the electron affinity for Cl is denoted by Δ.[65] The numerical values for the parameters are compiled in Table I.

For the pure covalent curve $\mathcal{H}^0_{11}(r) = V^0_C(r)$, a simple Morse potential is used

$$\mathcal{H}^0_{11}(r) = D_0\{\exp[-2a_0(r-r_0)] - 2\exp[-a_0(r-r_0)]\} \quad (4.2)$$

for which we need the three parameters D_0, a_0, and r_0. (The stretching force constant near the minimum for $\mathcal{H}^0_{11}(r)$ is given by $k_0 = 2a_0^2D_0$.) Since we have no detailed experimental information on these parameters, we follow the prescription introduced by Coulson and Danielsson[66] for hydrogen-bonding in water dimers and extended by Warshel and Weiss[23a] to enzyme systems. Thus for the pure covalent state bonding energy D_0, we use Pauling's geometric average, approximately 66 kcal/mol.[67] For the remaining two parameters r_0 and a_0, we assume that r_0 and the stretching force constant (i.e., $2a_0^2D_0$) are the same as the true

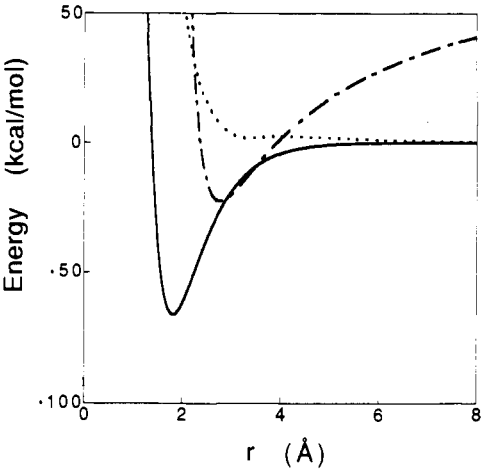

Figure 4. The vacuum Hamiltonian $\mathcal{H}^0(r)$ for *t*-BuCl in the orthonormal basis $\{\psi_C,\psi_I\}$: (—) vacuum covalent curve $V^0_C(r)$, (-·-) vacuum ionic curve $V^0_I(r)$, (···) electronic coupling $\beta(r)$. (Although not pursued here, it is of interest to note the crossing of the vacuum covalent and ionic curves.)

ground-state values, following Warshel and Weiss.[23a]

The true ground state for the gas-phase system, which is mainly a covalent state, can be well-approximated by a Morse potential

$$E_g(r) = D\{\exp[-2a(r-r_g)] - 2\exp[-a(r-r_g)]\} \quad (4.3)$$

which by using experimental data, we can determine completely [cf. Table I]. For *t*-BuCl, the dissociation energy D[68] and the equilibrium bond length r_g[69,70] are available. From the stretching force constant (=2.8 mdyne/Å),[70,71] we can also determine a = 1.58 Å^{-1}. We thus arrive at the r_0[72] and a_0 values for the pure covalent curve $\mathcal{H}^0_{11}(r)$ listed in Table I.

The electronic coupling $\mathcal{H}^0_{12}(r)$ is related to the pure covalent curve $\mathcal{H}^0_{11}(r)$, the pure ionic curve $\mathcal{H}^0_{22}(r)$, and the true ground-state potential energy $E_g(r)$ by

$$(\mathcal{H}^0_{11} - E_g)(\mathcal{H}^0_{22} - E_g) = (\mathcal{H}^0_{12} - E_gS)^2 \quad (4.4)$$

the secular equation for the gas-phase Schrödinger equation in the nonorthogonal diabatic basis $\{\phi_C, \phi_I\}$. For *t*-BuCl, we approximate the two diabatic wave functions as the two-electron spin-singlet states[73]

$$\phi_C \approx 2^{-1/2}[1 + \langle 2p_C\sigma|3p_{Cl}\sigma\rangle^2]^{-1/2}[2p_C\sigma(1)3p_{Cl}\sigma(2) + 2p_C\sigma(2)3p_{Cl}\sigma(1)]$$

$$\phi_I \approx 3p_{Cl}\sigma(1)3p_{Cl}\sigma(2) \quad (4.5)$$

where $2p_C\sigma$ and $3p_{Cl}\sigma$ are, respectively, the 2*p* carbon and 3*p* chlorine atomic orbitals with σ symmetry. With the approximation of Mulliken et al.,[74] the overlap integral $S(r)$ has a (positive) maximum at $r \approx 1.5$ Å.[75] By then noting that the overlap and the coupling usually have opposite signs,[60,76] we can determine

(65) For the electron affinity of Cl, we use 83.2 kcal/mol (Trainham, R.; Fletcher, G. D.; Larson, D. J. *J. Phys. B Lett.* **1987**, *20*, 777). With the value 154.5 kcal/mol reported by F. A. Houle and J. L. Beauchamp [*J. Am. Chem. Soc.* **1979**, *101*, 4067] for the adiabatic IP for *t*-Bu, the diabatic ionic potential $\mathcal{H}^0_{22}(r)$ goes below the true ground-state potential $E_g(r)$ [eq 4.3]. Since $\mathcal{H}^0_{22}(r)$ *cannot* be lower than $E_g(r)$, we shift $\mathcal{H}^0_{22}(r)$ up by increasing the IP by roughly 10 kcal/mol. See, also: Screttas, C. G. *J. Org. Chem.* **1980**, *45*, 333, where 159.7 kcal/mol is used for the IP for *t*-Bu.

(66) Coulson, C. A.; Danielsson, U. *Arkiv Fysik* **1954**, *8*, 245.

(67) Pauling, L. *The Nature of the Chemical Bonding*, 2nd ed.; Cornell University: Ithaca, NY, 1940; section 9a. When applied to *t*-BuCl with $D_{Cl-Cl} \simeq 59$ kcal/mol [Hubert, K. P.; Herzberg, G. *Molecular Spectra and Molecular Structure Constants of Diatomic Molecules*; Van Nostrand: New York, 1979] and $D_{Bu-Bu} \simeq 73$ kcal/mol [Griller, D.; Kanabus-Kaminska, J. M.; Maccoll, A. *J. Mol. Struct.* **1988**, *163*, 125], $D_0 = (D_{Cl-Cl}D_{Bu-Bu})^{1/2}$ gives $D_0 = 65\sim66$ kcal/mol.

(68) Cox, J. D.; Pilcher, G. *Thermochemistry of Organic and Organometallic Compounds*; Academic: London, 1970.

(69) Lide, D. R., Jr.; Jen, M. *J. Chem. Phys.* **1963**, *38*, 1504.

(70) Hüttner, W.; Zeil, W. *Spectrochim. Acta* **1966**, *22*, 1007.

(71) Graczyk, D. G.; Julian, R. L.; Taylor, J. W.; Worley, S. D. *J. Am. Chem. Soc.* **1975**, *97*, 7380.

(72) If we instead use Pauling's geometric mean $r_0 = (r_{Cl-Cl}r_{Bu-Bu})^{1/2}$ [cf. ref 67], we have $r_0 \simeq 1.75$ Å, which is rather close to r_g.

(73) Our sign convention for the two p-orbitals in eq 4.5 is such that the lobes in the region between *t*-Bu and Cl have positive signs. Thus ϕ_C is a bonding orbital, with a large electron density there.

(74) Mulliken, R. S.; Rieke, C. A.; Orloff, D.; Orloff, H. *J. Chem. Phys.* **1949**, *17*, 1248.

(75) The numerical value for $S(r)$ with the Slater-type orbitals[74] is ~0.36 at $r = 2$ Å and ~0.2 at $r = 2.5$ Å.

(76) Newton, M. D. *Int. J. Q. Chem. Symp.* **1980**, *14*, 363.

the coupling $\mathcal{H}^0_{12}(r)$ between the two pure diabatic states from eqs 4.1–4.4. We can then evaluate V^0_C, V^0_I, and β for the vacuum Hamiltonian in the orthonormal basis $\{\psi_C, \psi_I\}$ by using eq 2.6.

This completes our prescription for the Hamiltonian matrix elements in vacuum as a function of the RX separation r.[77] The numerical results are displayed in Figure 4. Notice that the electronic coupling β between the covalent and ionic states is rather large (i.e., $\gtrsim$15 kcal/mol) for $r \lesssim 2.5$ Å and varies rapidly with r. We will see below that due to this large coupling, there is a single stable well along the solvent coordinate as in Figure 3—a stark contrast to activated electron-transfer reactions.[78]

4.B. Solution Free Energy. With the gas-phase Hamiltonian determined above, we can now evaluate the reaction free energy surface for the ionic dissociation processes in solution, as a function of r and the solvent coordinate s by using the solution of eq 3.9 to evaluate 3.11. Here we will first explicitly consider three aprotic solvent systems, strongly polar acetonitrile (CH_3CN), weakly polar chlorobenzene (C_6H_5Cl), and nonpolar benzene (C_6H_6) and then consider in general an even broader range of solvent polarity.[79] The optical and static dielectric constants for C_6H_5Cl are $\epsilon_\infty \approx 2.33$ and $\epsilon_0 \approx 5.62$, while CH_3CN has $\epsilon_\infty \approx 1.81$ and $\epsilon_\infty \approx 35.94$.[80] For benzene, we use $\epsilon_\infty = \epsilon_0 \approx 2.27$.[80] (Since $\vec{P}_{or} = 0$ for benzene, there is no solvent coordinate and the "surface" is one-dimensional.) The two-dimensional reaction surfaces presented here and in part 2 differ from earlier efforts[17,18] by proper inclusion of the solvation-influenced S_N1 solute electronic structure.

We pause to remark on the obvious fact that water is certainly another interesting polar solvent system. However, there is a very significant entropy decrease when t-BuCl is solvated in water, associated with an increase in the ordering of the water molecules surrounding the solute ("structure-making").[3e,7a,8c,81] This increases the free energy associated with the initial t-BuCl *reactant* state by several kcal/mol, thus rendering the activation free energy significantly smaller than in other solvents. It is difficult to incorporate this patently microscopic, anomalous entropy effect into our dielectric continuum description, and thus water will not be considered here.[82] Although this entropy effect for other strongly hydrogen-bonded systems such as methanol is as small as in polar aprotic solvents,[11] a prudent view is that the dielectric continuum model is most reliable in a qualitative sense for aprotic solvents, and its direct application to polar protic solvents should be made with considerable reserve.

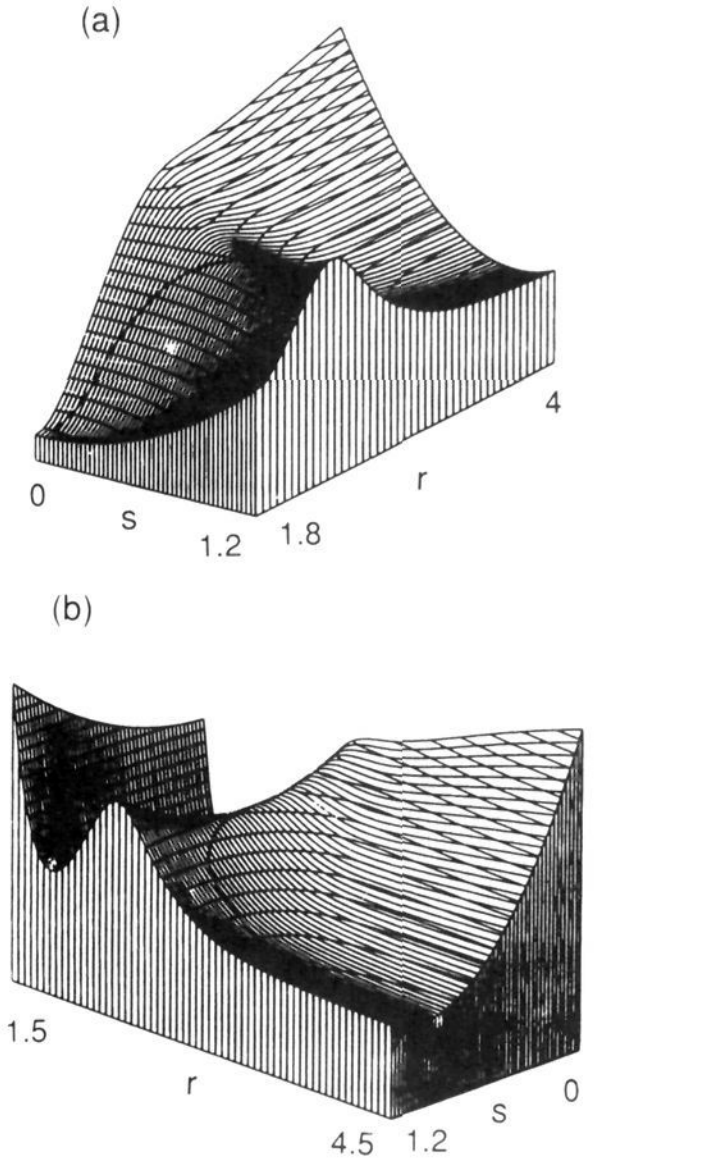

Figure 5. Free energy surface for t-BuCl in CH_3CN on the (r,s)-reaction coordinate system (r in Å), viewed (a) from the reactant side and (b) from the product side. The solid line connecting the reactant and product states through the saddle point is the equilibrium solvation path satisfying eq 3.12.

To calculate the free energy in solution, we first need the electrostatic energy $M_s(r)$, eq 2.10, associated with the solute electric field $\vec{\mathcal{E}}_I(\vec{x};r)$. Due to the mixing in ψ_I, i.e., the presence of small covalent character in the ionic state ψ_I [cf. eq 2.4], it is convenient to calculate first the self-energy

$$M^0_s(r) \equiv \frac{1}{8\pi}\int_V d\vec{x}\,\vec{\mathcal{E}}^0_I(\vec{x};r)\vec{\mathcal{E}}^0_I(\vec{x};r) \tag{4.6}$$

associated with $\vec{\mathcal{E}}^0_I(\vec{x};r)$ arising from the pure ionic state $\phi_I[R^+X^-]$, t-Bu^+ and Cl^-. We can then obtain $M_s(r)$ by

$$M_s(r) = [1 - S^2(r)]^{-2}M^0_s(r) \tag{4.7}$$

which is a direct consequence of eq 3.7. The self-energy $M^0_s(r)$ is evaluated in the two cavity description à la Marcus[45] for large separation

$$M^0_s(r) = e^2(1/2a_{Bu^+} + 1/2a_{Cl^-} - 1/r) \tag{4.8}$$

and then smoothly extrapolated to zero for a united atom according to Zichi and Hynes.[17,84] The cavity radii a_{Bu^+},a_{Cl^-} employed are 2.58 Å for t-Bu^+ and 1.81 Å for Cl^-. The latter value is just the crystal ionic radius for Cl^-; the former is chosen to obtain the correct ratio between the solvation free energies for t-Bu^+ and Cl^-.[85]

(77) If we change D_0 in $V^0_C(r)$, the electronic coupling $\beta(r)$ varies accordingly. For example, a smaller D_0 values yields a larger coupling $\beta(r)$ almost everywhere in r.

(78) The overlap integral $S(r)$ is also quite large for $r \lesssim 2.5$ Å. For $r \approx 1.8$ Å, S is about 0.4, yielding a rather significant mixing of the two nonorthogonal pure states $\phi_{C,I}$ in the ionic state ψ_I. Due to this admixture, the vacuum electric field $\vec{\mathcal{E}}_I$ arising from ψ_I becomes strengthened compared to $\vec{\mathcal{E}}^0_I$ by ~15% from eq 3.7. Near $r = 2.4$ Å, S is less than $^1/_4$ and thus ψ_I is almost completely pure ionic; the relative difference between $\vec{\epsilon}_I$ and $\vec{\epsilon}^0_I$ is $\lesssim$6%. From this perspective, the solvent coordinate s very near the reactant state is not an appropriate measure for the equilibrium pure ionic state occupation [cf. eq 3.13]. However, this is not a restriction, but rather requires a simple reinterpretation for small r, viz., the proper pure ionic state occupation at the reactant state would be about 15% larger than s_{eq}. (Care should be taken in the interpretation of the pure ionic state occupation because the two pure states are *not* orthogonal. Here we use the pure ionic state occupation as the coefficient for ϕ^2_I when we express the nonequilibrium solvation state charge distribution Ψ^2 in the diabatic basis.) But in any event, these are very small numbers near the reactant. In analyzing the S_N1 transition state, any reinterpretation for s is unnecessary since ψ_I is almost purely ionic.

(79) For the limiting S_N1 process (in the sense of section 1) in certain aprotic solvents such as acetonitrile and benzene, there exist experimental data, where the rate for a mixture of aprotic solvents with alcohols is measured and extrapolated to zero alcohol concentration. [See ref 12a for acetonitrile and benzene and ref 1e for nitromethane.] For chlorobenzene, no such data exist to the best of our knowledge; the experimental activation free energy is for the E1 process in eq 1.3. We nonetheless include chlorobenzene in our calculations to provide a solvent of polarity intermediate between CH_3CN and C_6H_6.

(80) Reichardt, C. *Solvents and Solvent Effects in Organic Chemistry*, 2nd ed.; Verlag Chemie: Weinheim, 1988.

(81) Franks, F.; Reid, D. S. In *Water: A Comprehensive Treatise*; Franks, F., Ed.; Plenum: New York, 1973; Vol. 2.

(82) Another difficulty with a continuum model for water solvent is that the continuum solvent force constant [eq 2.15 for K^0_s] has an incorrect (increasing) trend as the t-BuCl ionizes [cf. refs 47d and 83].

(83) Keirstead, W.; Wilson, K. R.; Hynes, J. T. *J. Chem. Phys.* **1991**, *95*, 5256. Since $\hbar\omega_{el}$ for water is ~20 eV, ρ is $\lesssim$0.1 for this reaction, and the BO treatment in this reference is an appropriate approximation.

(84) There is a free energy change δG associated with cavity size variation as the two cavities begin to overlap. A very rough estimate based on the simple relation $\delta G = \gamma\delta A$ (γ = solvent surface tension; δA = cavity area change) shows that δG is less than 1 kcal/mol as r changes from 1.8 to 2.5 Å with $\gamma \approx 30$ dyne/cm. This is within the error involved in the united atom extrapolation explained in the text and thus will be ignored.

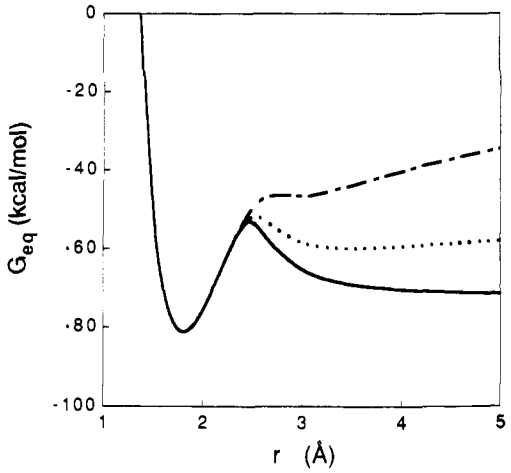

Figure 6. Equilibrium solvation free energy profile for *t*-BuCl heterolysis: (—) acetonitrile, (···) chlorobenzene, and (-·-) benzene.

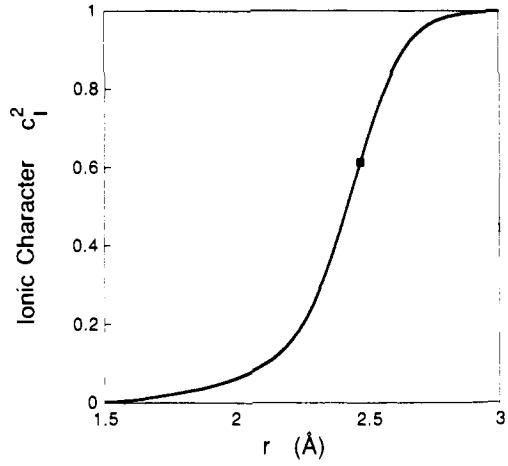

Figure 7. Charge distribution along the ESP in CH_3CN. The filled square denotes the transition state.

The calculated S_N1 ionization free energy surface for CH_3CN solvent is displayed in Figure 5 for illustration. We identify the local minima as the reactant and product states and saddle points as the transition state.[86] Since these extremum points satisfy eq 3.12, they are equilibrium solvation states, where both solvent polarizations are fully in equilibrium with the solute charge distribution. There are only two local minima and one saddle point in the S_N1 heterolysis, so that the reaction mechanism is unique. The dissociation can then be viewed as a barrier crossing starting from the minimum in the trench (reactant), passing through the minimum on the col (transition state) to the minimum located at infinite RX separation (product). The reactant state is located near $r = 1.8$ Å and $s \approx 0.05$ with relative free energy $G_R = -81$ kcal/mol. Since $s_{eq} = c_1^2$ from eq 3.13, the reactant is almost completely covalent.[87] The putative product state of completely dissociated ions is at $r = \infty$, though as discussed below, smaller separations are typically of interest. The saddle point located around $r \approx 2.47$ Å and ionic character $c_1^2 \approx 0.61$ with free energy $G^* \approx -53$ kcal/mol is the S_N1 transition state; the activation free energy $\Delta G^* = G^* - G_R$ is roughly 28 kcal/mol, which agrees remarkably well with experimental estimates.[88a,89,90] Note that at the transition state there is a well in the solvent coordinate. This feature, due to the strong electronic coupling, is in marked contrast to activated electron-transfer reactions, for which there is a barrier in the solvent coordinate. In the language of Pross and Shaik,[19-21] we would say that there is an electron shift rather than an electron transfer, accompanied by bond coupling. The solvent well characteristics will be discussed in more detail in part 2, where we discuss reaction paths on the two-dimensional free energy surface.

At any given r value, the *minimum* free energy is the equilibrium value $G_{eq}(r)$ for which $s = s_{eq} = c_1^2$. In fact this is the equilibrium solvation path, introduced in section 3 and indicated in Figure 5. The free energy $G_{eq}(r)$ is displayed versus RX separation in Figure 6 for CH_3CN solvent. The charge transfer character of the S_N1 ionization is particularly evident in the calculated ionic character c_1^2 along this ESP [Figure 7]. The charge shift is fairly rapid, being localized in a range of ≈0.25 Å. Nonetheless, this shift clearly does not have the singular abrupt Franck–Condon character[46] associated with activated electron transfer nor does it have the required isoenergetic character; as will be noted in part 2, there is a considerable free energy change (~10 kcal/mol) associated with the r change accompanying the shift in ionic character. Finally, Figure 7, with Figure 6, also indicates that separations near $r \approx 2.8$ Å correspond to a completely ionic ($c_1^2 \approx 1$) ion pair.

For the less polar C_6H_5Cl solvent [Figure 6], the reactant state location is the same as in acetonitrile, i.e., $r = 1.8$ Å and $s \approx 0.05$, a reflection of the predominantly covalent character of the reactant.[87] Probably the most salient difference between the two solvents is the appearance of a second local minimum for chlorobenzene at $r \approx 3.44$ Å and $s \approx 1$ with $G \approx -60$ kcal/mol; its ionic character is ≈100%. It is striking that our dielectric continuum model predicts the existence of an intimate ion pair for weakly polar solvents.[91] *t*-BuCl dissociates to an ion pair in C_6H_5Cl, rather than completely dissociating to *t*-Bu^+ and Cl^-, with the transition state at $r \approx 2.53$ Å, $s = c_1^2 \approx 0.67$ with a free energy $G^* \approx -51$ kcal/mol. The activation free energy ΔG^* is thus approximately 30 kcal/mol; the experimental value is about 33 kcal/mol.[88b] Thus, the calculated barrier height decrease from chlorobenzene to acetonitrile solvent is approximately 2 kcal/mol. The corresponding experimental change in ΔG^* is fairly close to this, about 3.6 kcal/mol.[11,92] One would conventionally view this decrease as due to the more potent solvent stabilization of the polar

(85) (a) The solvation free energy for *t*-Bu^+ is estimated from the heat of solvation ΔH_{solv} by assuming a linear relationship between ΔH_{solv} and the entropy of solvation. (b) The point charge location for *t*-Bu^+ in its spherical cavity is off-centered by 2.02 Å. Thus the closest approach between *t*-Bu^+ and Cl^- without cavity overlap is 2.37 Å [cf. ref 2b].

(86) If there are several minima and/or saddle points, they correspond to different reaction mechanisms and reaction routes.

(87) Our two-state model predicts that the *t*-BuCl electric dipole moment for the reactant state is 0.6–0.7 D, which is significantly smaller than the experimental value 2.13 D (see ref 69 and Sorriso, S.; Ricci, A.; Danieli, R. *J. Organomet. Chem.* **1975**, *87*, 61). Possible sources for this discrepancy include (1) inaccuracy associated with the strong repulsive part of the diabatic ionic curve $\mathcal{H}_{22}^0(r)$ eq 4.1 at small r, (2) hybridization of the 3*p* Cl orbitals with its nonbonding orbitals, (3) deviation of the *t*-Bu cation from planar geometry due to the sp^3 orbital hybridization, and (4) increase in the purely covalent and ionic states ϕ_C and ϕ_I overlap arising from this hybridization. (A homopolar dipole moment associated with ϕ_C is rather insignificant (~0.1 D) with Slater-type atomic orbitals for ϕ_C, following Mulliken et al.)[74] We believe that first and second sources are most important. We estimate that the reactant dipole moment discrepancy will lead to reduced ΔG^* with errors of ~0.7 kcal/mol for low polarity solvents and ~1.5 kcal/mol for highly polar solvents.

(88) (a) If we use 19.49 kcal/mol for ΔG^* in water [ref 7a] and combine it with 9.74 kcal/mol for ΔG^* (in acetonitrile) – ΔG^* (in water) reported in ref 11e, we obtain $\Delta G^* = 29.23$ kcal/mol for CH_3CN. (b) Similarly ΔG^* for chlorobenzene becomes 32.86 kcal/mol.

(89) In polar and nonpolar aprotic solvents, the olefin-forming elimination process is believed to follow the rate-determining unimolecular ionization step, as discussed in section 1. The experimental activation free energies in such solvents are estimated by measuring the rate for either the olefin formation or the acid development [cf. eq 1.3]. See refs 12 and 13.

(90) As detailed in section 3 of part 2, differences of ~1 kcal/mol between predicted ΔG^* values and those inferred from experiment are to be expected a priori.

(91) It is interesting to observe that the theoretical establishment of all solvent-separated ion pairs to date has required a *molecular* theory for the solvent. See, e.g., ref 64 and the extensive reference list: Ciccotti, G.; Ferrario, M.; Hynes, J. T.; Kapral, R. *J. Chem. Phys.* **1990**, *93*, 7137.

(92) Experimentally, this change in G^* is measured by observing the acid formation rate from the dissociated ions or ion pairs—acid formation is fast compared to the ionic dissociation process.[11] Once the ion pairs or dissociated ions are formed via the S_N1 mechanism from mainly covalent reactant *t*-BuCl, they are rapidly intercepted by a base such as pyridine present in the system. The rate constant at vanishing base concentration is then obtained by extrapolation.

transition state with increasing solvent polarity; we will see about this in section 5.

It is interesting to observe that experimental $\Delta G^{\ddagger}$ values in highly nonpolar solvents such as benzene lie only a few kcal/mol above the polar solvent values—a somewhat surprisingly small change given the solvent polarity difference. To be more specific, $\Delta G^{\ddagger}$ increases only by 4.7 kcal/mol from acetonitrile to benzene.[11,12] To compare with this, we have carried out a free energy calculation for benzene with $\epsilon_\infty = \epsilon_0 \approx 2.27$, shown in Figure 6. The reactant state is located at $r \approx 1.8$ Å as before. The transition state is located at $r \approx 2.75$ Å with $s \approx 0.89$ and $G^{\ddagger} \approx -46$ kcal/mol. Thus the activation free energy increase from acetonitrile to benzene in our model is approximately 7 kcal/mol. Again there is a second minimum—rather broad and flat—around $r \approx 3$ Å with free energy $G \approx -47$ kcal/mol, corresponding to an intimate ion pair, as in chlorobenzene. The ionic character for this species is $c_1^2 \approx 1$.

Our prediction of locally stable *t*-Bu^+Cl^- ion pairs in weakly polar (C_6H_5Cl) and even nonpolar solvents (benzene) is of particular interest. Ingold[1f] was among the first to strongly emphasize the possibilities for heterolytic polar reactions in such solvents. Our results basically support those views—in particular the absence of the necessity to form completely separated ions. The existence of an intimate ion pair arises from the competition between the attractive part of the gas-phase ionic potential and the solvent stabilization favoring the full charge separation in solution (which thus is repulsive).[17,93] In a weakly polar solvent this stabilization is small; it does not overcome the gas-phase attractive potential at large separations. Thus instead of monotonically decreasing [cf. Figure 1b], G_1^{eq} has a minimum around $r \approx 3$–4 Å for a weakly polar solvent.[94] Further, the predicted contact ion pair local minima indicate some stability against collapse to covalent *t*-BuCl.

Our results also make it clear that the collapse[7b,10a,b,21b,95] of this ion pair to the covalent *t*-BuCl is opposed by a free energy barrier associated with the cost to change the solvation from that of the fully ionic pair to that of the less intensely charged transition state and from that of the larger separated ion pair to that of the tighter transition state.[96]

As explained in section 4A, these S_N1 ionizations are in the strong electronic coupling regime where there is *no* barrier in the solvent at the transition state.[30a,b] In this regime, the solvent electronic polarization $\vec{P}_{el}$ can make a free energy contribution almost as significant as the solvent orientational polarization.[30] Near the transition state $\Delta G_r^{el}/4$ is about 4 kcal/mol; since its contribution to the activation free energy is scaled down by a factor[27] $f = \rho/(2c_C c_1 + \rho)$ [eq 3.1] and ρ is not that small ($\rho \approx 0.3$), its contribution is approximately 1 kcal/mol for both CH_3CN and C_6H_5Cl solvents because $\epsilon_\infty \approx 2$ and the transition-state structure is similar for both solvents. In weakly polar chlorobenzene, the $\vec{P}_{el}$ contribution to the activation free energy is about 50% of that from $\vec{P}_{or}$ (≈2 kcal/mol). This $\vec{P}_{el}$ contribution of ≈1 kcal/mol is almost 35% of the total solvent contribution (≈3 kcal/mol) for C_6H_5Cl, while it is about 20% of the total solvent contribution (≈5 kcal/mol) for more polar CH_3CN. (In the SC approximation, the $\vec{P}_{el}$ contribution is ≈2 kcal/mol for both solvents.) (There is of course no $\vec{P}_{or}$ contribution at all for benzene solvent.) This nonnegligible contribution of $\vec{P}_{el}$ is totally missing if a standard (BO) diagonalization of the two diabatic states is made [cf. discussion below eq 3.15].

A final aspect of especial interest in this initial survey is the tightness ($r^{\ddagger}$) and the extent of the ionic character ($c_1^{\ddagger 2}$) at the transition state with changing solvent polarity. As we change from acetonitrile to benzene, the $r^{\ddagger}$ value increases from 2.47 to 2.75 Å. For acetonitrile, $c_1^{\ddagger 2} \approx 0.61$ so that the transition state is approximately 61% ionic. By contrast, for weakly polar chlorobenzene, $c_1^{\ddagger 2} \approx 0.67$, and for nonpolar benzene, $c_1^{\ddagger 2} \approx 0.89$. Thus the transition state becomes *less* ionic and *more* tight with increasing solvent polarity. This seemingly bizarre feature is taken up next.

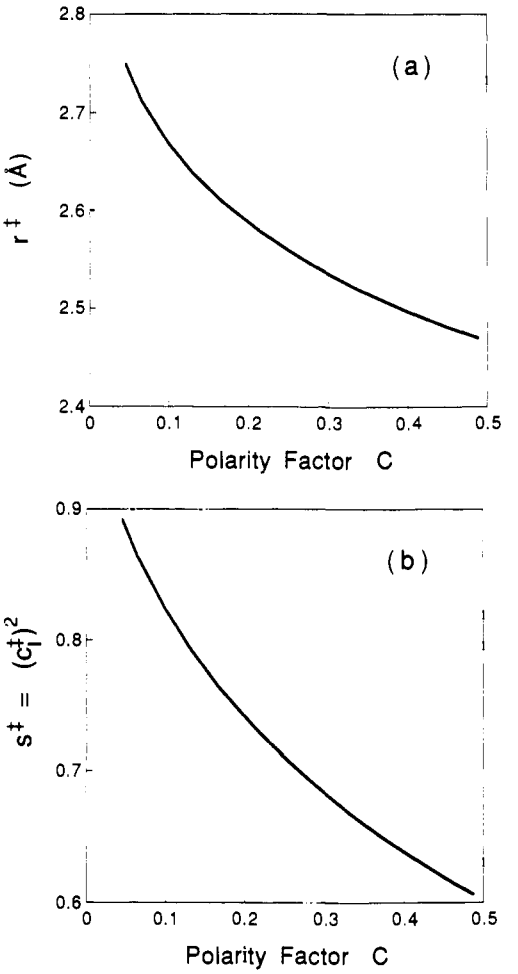

Figure 8. The *t*-BuCl ionization transition-state structure variation with solvent polarity factor $C = \epsilon_\infty^{-1} - \epsilon_0^{-1}$: (a) RX separation $r^{\ddagger}$ and (b) charge character $s^{\ddagger} = c_1^{\ddagger 2}$.

5. Analysis for General Solvent Polarity

In the previous section, we studied *t*-BuCl S_N1 ionizations in acetonitrile, chlorobenzene, and benzene. The numerical results for these three solvents show that the free energy $G^{\ddagger}$, the ionic character $s^{\ddagger} = c_1^{\ddagger 2}$, and the internuclear separation $r^{\ddagger}$ at the transition state all decrease, at differing rates, with increasing solvent polarity. We now analyze these features in some detail from a general perspective. To keep our analysis and interpretation as simple and clear as possible, we assume in what follows that $\epsilon_\infty = 2$ independent of the solvent.

5.A. Transition-State Structure. The first aspect that we investigate is the transition-state location ($r^{\ddagger}$, $s^{\ddagger}$) and its change with solvent polarity. We remind the reader that for equilibrium solvation states, $s_{eq} = c_1^2$ [eq 3.13] and thus $s^{\ddagger}$ denotes precisely how ionic the transition state is. Since the transition state is the saddle point on the free energy surface, it can be located analytically by investigating the first and second derivatives of the free energy. The first-order derivatives vanish at the transition state. Omitting all the complex details concerning the derivatives, we summarize our numerical results in Figure 8. There it is seen that both $r^{\ddagger}$ and $s^{\ddagger}$ decrease as the solvent becomes more polar; *the transition state becomes more covalent and tight as the solvent polarity increases*. This key result may appear to be counterintuitive at first sight and certainly contradicts various statements in the literature.[8d,11,16a,97,98] But we can in fact understand this

(93) Warshel, A. *J. Phys. Chem.* **1979**, *83*, 1640.

(94) Such an intimate ion pair minimum appears in Figure 1 of ref 19a and Figure 14 of ref 20a, although it is neither derived nor is its origin explained.

(95) (a) Kessler, H.; Feigel, M. *Acc. Chem. Res.* **1982**, *15*, 2. (b) Masnovi, J. M.; Kochi, J. K. *J. Am. Chem. Soc.* **1985**, *107*, 7880. (c) Paradesi, C.; Bunnett, J. F. *J. Am. Chem. Soc.* **1985**, *107*, 8223.

(96) This is somewhat offset by the increase in electron coupling for the more compact transition state, whose contribution lowers the barrier for internal return. (See section 5B.)

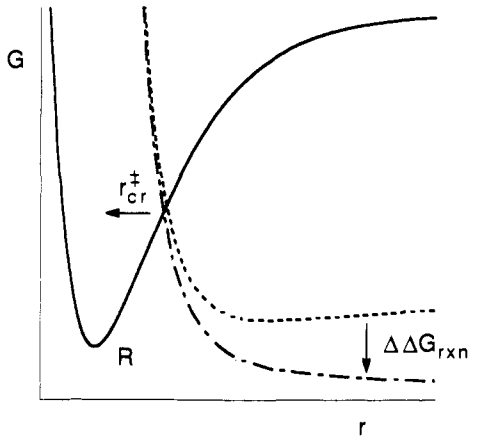

Figure 9. Hammond postulate diagram. The covalent state free energy G_C^{eq} is denoted by (—). The solvent equilibrated ionic curves G_I^{eq} for CH_3CN and C_6H_5Cl are represented by (–·–) and (···), respectively. As the solvent polarity increases, the reaction becomes less endothermic ($\Delta G_{rxn} > 0$); the crossing point denoted as $r^{\ddagger}_{cr}$ diminishes in the direction of the reactant state R.

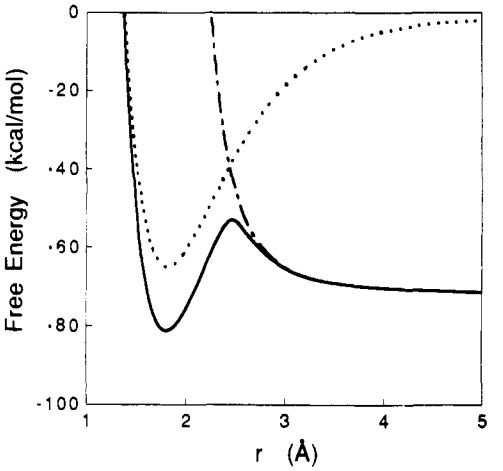

Figure 10. Free energy profiles for equilibrated adiabatic and diabatic states for acetonitrile: (—) G_{eq}, (···) G_C^{eq}, and (–·–) G_I^{eq}.

at least qualitatively at this stage in terms of the Hammond postulate[99] (or the Bell–Evans–Polanyi principle[100]) as follows. With increasing solvent polarity, the ionic state becomes more stabilized, and thus the dissociation becomes more exothermic (here, less endothermic) [Figure 9]. According to the Hammond postulate, with increasing exothermicity the transition-state character approaches that of the reactant, which is the tightly bound, covalent state (r = 1.8 Å and $s \approx 0.05$) compared to the product (either dissociated ions or ion pair, for which $r \gg 1.8$ Å and $s \approx 1$). But we will see presently that a considerably deeper analysis is in fact required to properly understand the trends in the transition-state ionic character.

Discussion of the transition-state geometry, i.e., the separation $r^{\ddagger}$, is not simple, and the reasons for the deviations from the simple Ogg–Polanyi picture $r^{\ddagger} = r_{cr}$ described in section 2 are manifold. To see whether the crossing point r_{cr} between the two free energy curves, G_C^{eq} and G_I^{eq}, in eq 2.11 coincides with the transition-state separation $r^{\ddagger}$, we have displayed in Figure 10 G_C^{eq}, G_I^{eq} and the equilibrium free energy G_{eq} along the ESP as a function of r, with the solvent coordinate at its equilibrium value $s = s_{eq} = c_I^2$. This shows that $r^{\ddagger}$ is slightly larger than the crossing point separation. This is mainly due to the fact that the electronic coupling $\beta(r)$ between the covalent and ionic states decreases with increasing r [cf. Figure 4]; the lower curve in the region $r > r_{cr}$ becomes significantly less stabilized than $r < r_{cr}$; the location of the maximum on the lower adiabatic curve thus shifts to a larger value of r compared to r_{cr}. Due to this small but critical shift, a simple crossing point analysis of the transition-state ionic character c_I^2—which always gives 50% as noted in section 2—can be in significant error, owing to the very rapid variation of c_I^2 with r illustrated in Figure 7 [ref 101]. This already alerts us to the feature that the transition-state ionic character is a result of several contributing factors.

As can be seen from Figure 8a, the RX separation $r^{\ddagger}$ at the transition state decreases for more polar solvents, a direction consistent with the Hammond postulate, illustrated in Figure 9. However, this change is small—in the range $3 \leq \epsilon_0 \leq 80$, the relative change in $r^{\ddagger}$ is only about 5%. This truculence vis-à-vis the solvent can be attributed to two features: first, the vacuum potentials $V_I^0(r)$ and $V_C^0(r)$, are close to each other near $r = r^{\ddagger} \simeq$ 2.5 Å; second, the covalent curve $V_C^0(r)$ is rather steep in that region. Under these conditions the differing solvent stabilization of the ionic state for different solvent polarity affects the r-value for the crossing point only in a minor fashion. Since $r^{\ddagger}$ is close to this crossing point, we thus expect a small change in $r^{\ddagger}$ with solvent polarity—a feature noted in section 4B. This is also basically why the change noted there in $\Delta G^{\ddagger}$ with solvent polarity is small despite the importance of the solvation to the very existence of the transition state. But the most critical point for our further discussion is the feature that $r^{\ddagger}$ *decreases with increasing solvent polarity*.

We next consider the transition-state free energy $G^{\ddagger}$ and its correlation with the solvent polarity. To investigate this, we take the derivative of $G^{\ddagger}$

$$\frac{dG^{\ddagger}}{dC} = \frac{\partial G^{\ddagger}}{\partial C} + \frac{\partial G^{\ddagger}}{\partial s^{\ddagger}}\frac{ds^{\ddagger}}{dC} + \frac{\partial G^{\ddagger}}{\partial r^{\ddagger}}\frac{dr^{\ddagger}}{dC}$$

$$= \frac{\partial G^{\ddagger}}{\partial C} \qquad (5.1)$$

$$= -s^{\ddagger 2} M_s(r^{\ddagger})$$

with respect to the (Pekar[102]) solvent polarity factor C measuring the solvation via the solvent orientational polarization

$$C \equiv \frac{1}{\epsilon_\infty} - \frac{1}{\epsilon_0} \qquad (5.2)$$

The (positive) factor M_s is defined in eq 4.7, and, in going from the first line to the second of eq 5.1, we have used the fact that at the transition state the first r and s derivatives of the free energy vanish. Thus $G^{\ddagger}$ diminishes with increasing solvent polarity, and so does the activation free energy $\Delta G^{\ddagger} = G^{\ddagger} - G_R$ since the reactant free energy G_R remains nearly constant, yielding a smaller activation free energy. This trend is, of course, just that expected from simple considerations of transition-state stabilization[1-18] and the one found in section 4B for three specific solvents. But this trend occurs *despite* the decreasing ionic character of the transition state, a signal that the fundamental origins of $\Delta G^{\ddagger}$ may be more complex than traditionally conceived; indeed we will demonstrate in section 5B that this is the case.

The striking trend of the transition-state ionic character $c_I^{\ddagger 2}$—decreasing charge development at the transition state with increasing solvent polarity—requires close scrutiny. As noted

(97) Clarke, G. A.; Taft, R. W. *J. Am. Chem. Soc.* **1962**, *84*, 2295.
(98) (a) Hoffmann, H. M. R. *J. Chem. Soc. (London)* **1965**, 6762. (b) Hoffmann, H. M. R.; Maccoll, A. *J. Am. Chem. Soc.* **1965**, *87*, 3774.
(99) Hammond, G. S. *J. Am. Chem. Soc.* **1955**, *77*, 334. For other applications of the principle to S_N1 reactions, see ref 6, and: Hoz, S. In *Nucleophilicity*; Harris, J. M., McManus, S. P., Eds.; ACS: Washington, DC, 1987.
(100) (a) Bell, R. P. *Proc. Roy. Soc. (London)* **1936**, *A154*, 414. (b) Evans, M. G.; Polanyi, M. *Trans. Faraday Soc.* **1938**, *34*, 11.
(101) This feature also has potential consequences for the transition state in other reaction classes;[19-22] its structure and charge distribution may depend upon the geometry along the reaction coordinate via the reaction coordinate-dependent electronic coupling. This aspect would then need to be accounted for in valence bond descriptions which predict[19] an equal (or nearly so) mixing of the reactant and product state electronic structures at the transition state.
(102) Pekar, S. I. *Untersuchungen über die Elektronentheorie der Kristalle*; Akademie-Verlag: Berlin, 1954.

above, a simple qualitative application of the Hammond postulate would predict that an earlier barrier crossing [cf. Figure 9] would indicate a more reactant-like (i.e., less ionic) transition state, which is precisely what we have found above. While this is correct in a general sense, in fact one *cannot* invoke a simple diabatic curve implementation, e.g., Figure 10, of the principle by itself to support the argument: A diabatic curve crossing analysis based on the valence bond description[2] given in section 2 clearly indicates that the transition state in such a description is *always* an *equal* mixture of the covalent and ionic states, i.e., a degenerate resonance hybrid; therefore, in this description the transition-state ionic character is incorrectly predicted to be $c_I^{\ddagger 2} = 0.5$ *irrespective* of the transition-state geometry, i.e., the $r^\ddagger$ value. (Pross and Shaik[19] have also generally pointed out that a simple two-state diabatic curve crossing analysis will yield a 50–50 mixture of states.) It is thus necessary to analyze $s^\ddagger = c_I^{\ddagger 2}$ in some detail to unravel the intriguing transition-state ionic character.

This program is carried out in the Appendix and we simply state here the net picture that emerges from the detailed analysis of this Appendix and the next section. Since the electronic coupling $\beta(r)$ is a decreasing function of r and thus better stabilizes the small r region, the actual transition-state location is more loose than the crossing point of the two equilibrated diabatic curves; as a result, the transition-state ionic character differs from, and is always more than, 50% ionic.[103] As the solvent polarity increases, the crossing point r value diminishes toward that of the reactant state. Among other things, this significantly increases the slope magnitude of the equilibrated diabatic ionic state, which in turn pushes the looser transition state closer to the diabatic crossing point. Thus with increasing polarity, the transition state tends to 50% ionic from above.

This can also be understood from a different viewpoint. Since the electronic coupling $\beta(r)$ is a decreasing function of r, the electronic coupling at the transition state thus increases with solvent polarity due to diminishing $r^\ddagger$. This coupling effect can be best utilized if the transition-state charge distribution becomes more delocalized (i.e., $2c_Cc_I \rightarrow 1$) so that the free energy is reduced [eq 3.11]; the covalent-ionic state coupling favors a mixed state, tending toward 50% ionic.[103] This can be attained only at the expense of the solvation free energy, whose stabilization effect decreases with a more delocalized charge distribution. For our model *t*-BuCl system, the r-dependence of the electronic coupling is much stronger (approximately exponential) than that of the solvation free energy; the gain in stabilization, i.e., depression of the barrier, via the electronic coupling with charge delocalization thus exceeds the loss due to the destabilization in solvation.[103] The transition-state ionic character, i.e., the charge separation, thus is reduced with increasing solvent polarity.

5.B. Activation Barrier Origin. We now explicitly analyze the influence of the solute electronic structure and the solvation on the S_N1 ionization activation free energy. To this end, we recall eqs 3.14 and 3.15, which we repeat here for convenience, specialized to the transition state

$$\Delta G^\ddagger = (V_C^0 c_C^{\ddagger 2} + V_I^0 c_I^{\ddagger 2} - k_B T \ln [r^\ddagger/r_0]^2 - G_R^{eq}) - 2\beta c_C^\ddagger c_I^\ddagger + \Delta G_{\ddagger,solv}^{eq}$$

$$\Delta G_{\ddagger,solv}^{eq} = -\Delta G_r^{el} s^\ddagger - \Delta G_r s^{\ddagger 2} + f^\ddagger \Delta G_r^{el} s^\ddagger (1 - s^\ddagger)$$

$$\simeq -\Delta G_r^{el} s^\ddagger - \Delta G_r s^{\ddagger 2} = -\left(1 - \frac{1}{\epsilon_\infty}\right) M_s c_I^{\ddagger 2} - \left(\frac{1}{\epsilon_\infty} - \frac{1}{\epsilon_0}\right) M_s c_I^{\ddagger 4} \quad (5.3)$$

where all quantities are evaluated at $r = r^\ddagger$. The approximate equality, displayed for clarity, follows when the BO approximation, i.e., $\rho = 0$ (and thus $f = 0$) is used since $\rho \approx 0.3$ while $y = 2c_Cc_I \approx 1$ at the transition state. The activation free energy comprises (a) the average of the vacuum covalent and ionic curves, minus the reactant free energy, (b) an electronic coupling contribution which diminishes $\Delta G^\ddagger$, and (c) an equilibrium solvation free energy. It is important to stress at the outset that in the conventional Hughes–Ingold explanation.[1h,16a,80,104] the decrease of $\Delta G^\ddagger$ with increasing solvent polarity would have its origin in $G_{\ddagger,solv}^{eq}$,

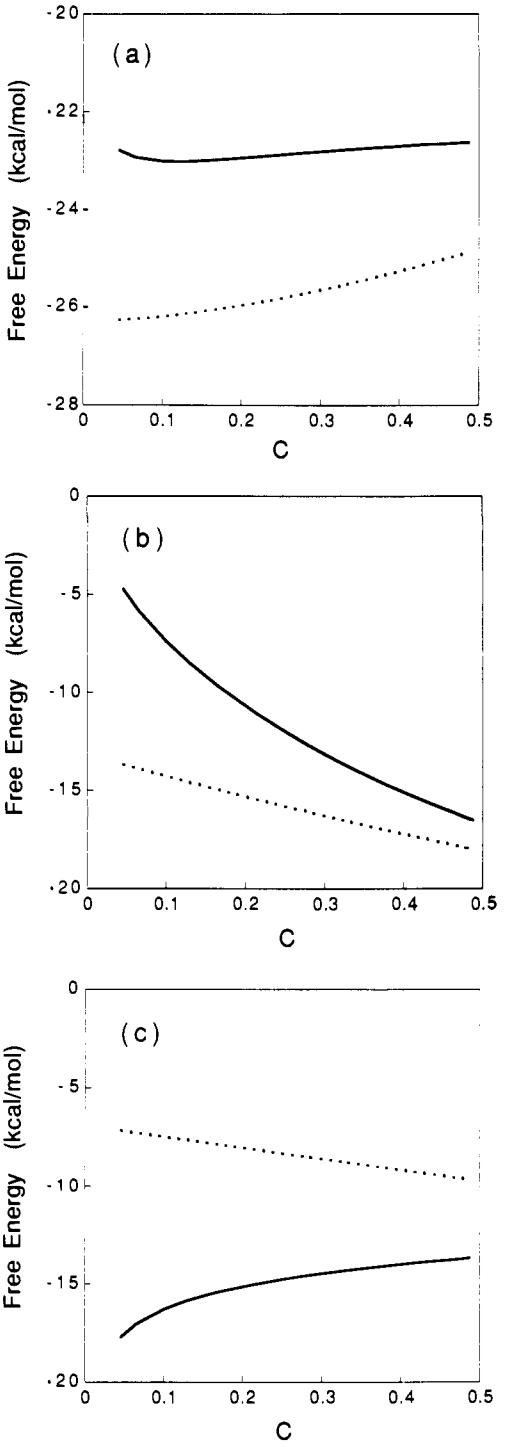

Figure 11. Dissected components of the activation free energy: (—) actual transition state, (···) diabatic crossing point, (a) weighted average of gas-phase curves, (b) electronic coupling contribution, and (c) transition-state solvation free energy.

(103) For weak coupling cases such as *t*-BuI, it is the vacuum diabatic energy difference $V_I^0 - V_C^0$ (and not the coupling) that is best utilized in stabilizing the transition state. For such systems, the transition-state ionic character can decrease below 50% ionic with increasing solvent polarity. The diminishing solvation contribution to the activation barrier and decreasing transition-state ionic character with growing solvent polarity—trends found for strongly coupled *t*-BuCl in the current work—remain intact even for weak coupling cases. For discussion of all these points, see: Mathis, J. R.; Kim, H. J.; Hynes, J. T. To be submitted for publication.

(104) Kosower, E. M. *An Introduction to Physical Organic Chemistry*; Wiley: New York, 1968.

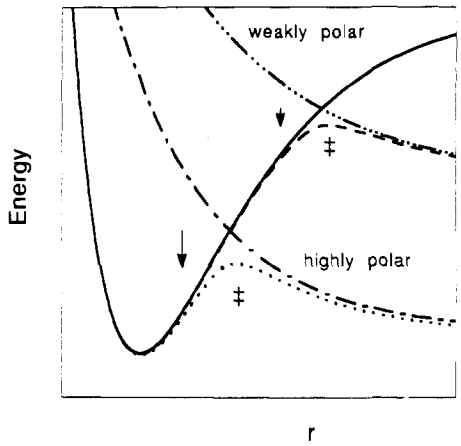

Figure 12. Schematic diagram for electronic coupling contribution to $\Delta G^{\ddagger}$. The diabatic covalent curve is denoted by —, while the (equilibrated) diabatic ionic curves for weakly and highly polar solvents are represented by (−···−) and (−·−), respectively. The corresponding adiabatic states are denoted by (−−−) and (···). The magnitude of the coupling stabilization of the transition state is indicated by an arrow and reflects the feature described in text that as solvent polarity increases, the transition-state separation $r^{\ddagger}$ decreases and the coupling increases.

i.e., an increasingly better solvent stabilization of the transition state.

These three ingredients are displayed in Figure 11 for a wide range of solvent polarity. The first component is nearly constant, and we do not discuss it further. The trend of the solvation $\Delta G^{eq}_{\ddagger,solv}$ contribution is initially surprising and contradicts conventional views: the transition-state solvation stabilization *decreases* as the solvent polarity increases. While the solvation free energy ΔG^{eq}_{solv} ($r = r^{\ddagger}$, $s = c_1^2 = 1$) for a full ion pair at $r = r^{\ddagger}$ indeed becomes more favorable (i.e., more negative) in this direction, the transition-state ionic character decreases—as documented in detail above—and the barrier rises in consequence [Figure 11c]. *The overall reduction in $\Delta G^{\ddagger}$ with increasing polarity thus proves to arise from an unexpected source—the trend of the electronic coupling contribution.* This arises as follows. As the transition-state location $r^{\ddagger}$ decreases with growing solvent polarity [cf. Figure 8a], the electronic coupling β increases exponentially and in consequence suppresses the ionization barrier [Figure 11b]. This effect is qualitatively illustrated in Figure 12. The associated increase of the delocalization of the electronic distribution produces a less ionic transition state.

This electronic coupling dominance scenario for $\Delta G^{\ddagger}$ contrasts with all previous descriptions for the S_N1 ionization of which we are aware. Indeed the electronic coupling plays no role at all in those discussions. Instead, it has been the conventional picture[1-18,80,104] that the $\Delta G^{\ddagger}$ solvent polarity trend is exclusively associated with more favorable solvation free energetic stabilization of the transition state, conventionally conceived of as more highly ionic in more polar solvents.[103]

The surprising trend of the equilibrium solvation free energy $\Delta G^{eq}_{\ddagger,solv}$ with respect to the solvent polarity factor C—which contradicts the Hughes-Ingold[1h,16a,80,104] rationale of transition-state solvation stabilization—is in particular worth some further inspection. If we differentiate the former with respect to the latter, we find, using the BO approximation for simplicity,

$$\frac{d}{dC}\Delta G^{eq}_{\ddagger,solv} = M_s\left[s^{\ddagger 2} + \frac{\partial\Lambda}{\partial s^{\ddagger}}\frac{ds^{\ddagger}}{dC} + \Lambda\frac{1}{M_s}\frac{\partial M_s}{\partial r}\frac{dr^{\ddagger}}{dC}\right] \quad (5.4)$$

$$\Lambda(s^{\ddagger}) \equiv \left(1 - \frac{1}{\epsilon_\infty}\right)s^{\ddagger} + \left(\frac{1}{\epsilon_\infty} - \frac{1}{\epsilon_0}\right)s^{\ddagger 2}$$

Since $dr^{\ddagger}/dC$ and $ds^{\ddagger}/dC$ are usually negative as noted above, the trend for the transition-state solvation free energy with C depends upon how rapidly the transition state—both its ionic character and location—varies with solvent polarity. The change in the ionic character is the more important factor, since $r^{\ddagger}$ varies

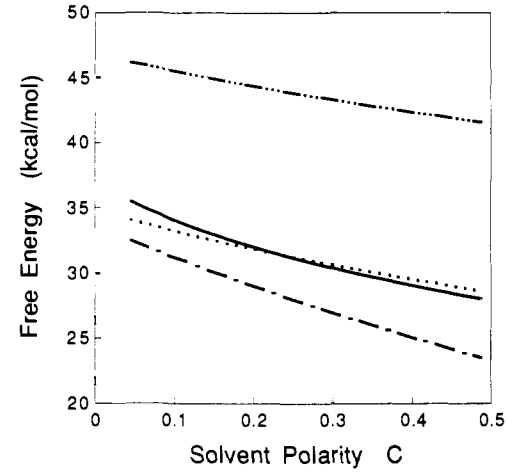

Figure 13. Activation free energy calculated from the crossing point: (—) the actual activation free energy $\Delta G^{\ddagger}$; (−···−) $\Delta G^{\ddagger}_{cr}$; (−·−) $\Delta G^{\ddagger}_{cr} - \beta$; and (···) $\Delta G^{\ddagger}_{cr} - \beta + {}^1/_4\,(\rho\Delta G^{el}_r + \Delta G_r)$. As expected from the discussion in text, the deviation increases for more weakly polar solvents.

little with solvent polarity. If $s^{\ddagger}$ depends sufficiently strongly on C so that the term in the square bracket in eq 5.4 is negative, the magnitude of $\Delta G^{eq}_{\ddagger,solv}$ *decreases* with increasing solvent polarity; this is in fact what we observe for the model *t*-BuCl system in a polar solvent [Figure 11c].[105] If we rewrite eq 5.4 by combining with eq 5.1, we obtain

$$\frac{d\Delta G^{\ddagger}}{d|\Delta G^{eq}_{\ddagger,solv}|} = -\left[1 + \frac{1}{s^{\ddagger 2}}\frac{\partial\Lambda}{\partial s^{\ddagger}}\frac{ds^{\ddagger}}{dC} + \frac{\Lambda}{s^{\ddagger}M_s}\frac{\partial M_s}{\partial r}\frac{dr^{\ddagger}}{dC}\right]^{-1} \quad (5.5)$$

which, with the discussion above, also shows quite clearly that the dependence of $\Delta G^{\ddagger}$ on the solvation free energy is of the opposite sign (positive) to conventional expectations. (The same conclusion follows from a similar but more complex discussion for the full form of $\Delta G^{eq}_{\ddagger,solv}$ in eq 5.3.)

With the key ingredients of the activation barrier established, we can also ask how a simple curve crossing analysis would fare in predicting $\Delta G^{\ddagger}$. In Figure 13 we plot the "conventional" activation free energies $\Delta G^{\ddagger}_{cr} - \beta$ [cf. section 2] and the actual activation free energies against solvent polarity. The free energy difference $\Delta G^{\ddagger}_{cr}$ between the reactant state and the crossing point of the two solvent-equilibrated uncoupled diabatic curves G^{eq}_{CI} [cf. eq 2.11] lies about 10 kcal/mol above the actual activation free energy $\Delta G^{\ddagger}$. By taking into account the electronic coupling between the two equilibrated diabatic curves at the crossing point, one obtains the conventional activation barrier $\Delta G^{\ddagger}_{cr} - \beta$, which is located well below $\Delta G^{\ddagger}$. The solvent-equilibrated valence bond method thus predicts a considerably lower activation barrier. This discrepancy arises from the fact that the solute electronic structure is a mixture of covalent and ionic states, i.e., a charge-delocalized state,[30] and that the solvent-equilibrated valence method does *not* treat this delocalization effect properly, i.e., the solvent reorganization is not taken into account [cf. section 2]. We can show from eqs 2.11, 2.12, and 3.11 by a perturbation expansion about the crossing point that

$$\Delta G^{\ddagger} \approx \Delta G^{\ddagger}_{cr} - \beta + \frac{1}{4}(\rho\Delta G^{el}_r + \Delta G_r) + \delta\Delta G^{\ddagger} \quad (5.6)$$

$$\delta\Delta G^{\ddagger} = \left(s^{\ddagger} - \frac{1}{2}\right)^2\left[2\beta - \left(\frac{\rho}{2}\Delta G^{el}_r + \Delta G_r\right)\right]$$

where all terms are evaluated at the crossing point, and the small

(105) Since there is a competition involved, we cannot rule out a priori the possibility that in some systems, $|\Delta G^{eq}_{\ddagger,solv}|$ will increase with solvent polarity.[106] In such a case, the drop in $\Delta G^{\ddagger}$ with solvent polarity would arise both from electronic coupling and solvation free energy effects.

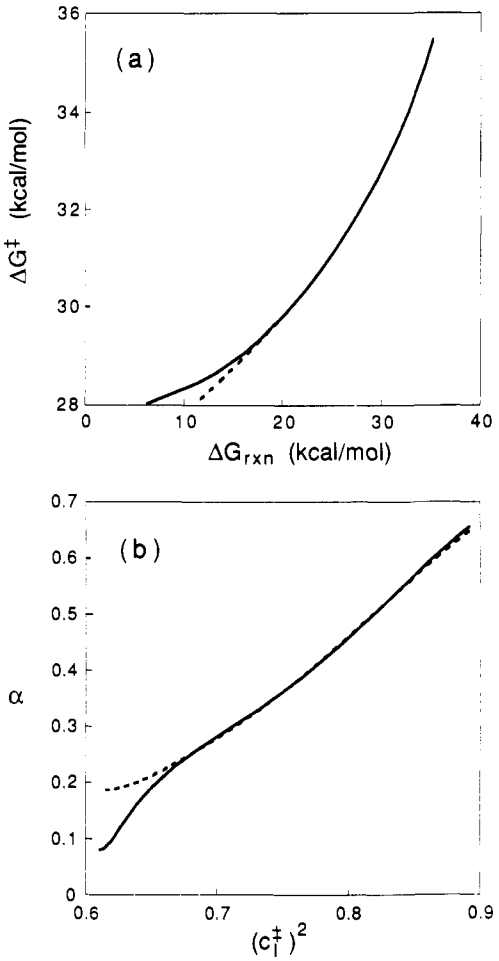

Figure 14. (a) Brønsted plot for activation and reaction free energies. (—) corresponds to ionizations to stable product states while (···) denotes the decomposition into an intimate ion pair (i.e., $r \lesssim 3.5$ Å). (b) The Brønsted coefficient α vs the transition-state ionic character plot. An almost linear correlation between the two holds for a wide solvent polarity range ($2.5 \lesssim \epsilon_0 \lesssim 80$).

difference $r^‡ - r_{cr}$ is neglected. The third term on the right-hand side of the equation for $\Delta G^‡$ is the solvent destabilization[107] arising from the maximal charge delocalization. Note the presence of the electronic polarization contribution $\rho\Delta G_r^{el}/4$, whose significance we have stressed in section 4B, in contrast to the simple crossing point estimation for $\Delta G^‡$ in eq 2.21. The final term $\delta\Delta G^‡$ accounts for the deviation of the actual transition-state charge distribution from the naive crossing value $c_1^2 = {}^1/_2$. Near the crossing point, and thus near the transition state, both 2β and M_s [eq 2.10] are about 30 kcal/mol. For nonpolar solvents (i.e., $\epsilon_0 \approx \epsilon_\infty \approx 2$), $2\beta - \rho\Delta G_r^{el}/2 - \Delta G_r$ is about 20 kcal/mol, and it decreases with growing solvent polarity [cf. eqs 2.13 and 2.14]. In addition, $(s^‡ - {}^1/_2)^2$ is $\lesssim 0.1$ for a wide range of solvent polarity ($\epsilon_0 \gtrsim 3$). Therefore $\delta\Delta G^‡$ can be safely ignored from a purely numerical point of view, and the actual activation free energy becomes approximately the sum of the diabatic equilibrated curve crossing activation free energy, corrected by the coupling, and the maximal solvent destabilization due to the charge delocalization. The agreement between the approximate expression with $\delta\Delta G^‡$ ignored and the actual $\Delta G^‡$ is truly remarkable in view of the former's fundamental shortcomings. For it must be stressed that the accuracy of the approximate form depends on very significant cancellation of errors in the three ingredients of $\Delta G^‡$ and—most importantly—misses the unconventional trend of the solvation ingredient per se [cf. Figure 11c]. Further, we have already established in section 5A that the crossing point analysis fails to accurately characterize the transition state ionic character.

5.C. Linear Free Energy Relations. i. Brønsted and Marcus Relations. Finally, we consider the applicability of simple linear free energy relationships (LFER) for the S_N1 ionization. In particular, we consider an empirical relation connecting the kinetics and equilibrium, i.e., the Brønsted relation

$$\Delta\Delta G^‡ = \alpha\Delta\Delta G_{rxn} \tag{5.7}$$

with varying solvent polarity. Here ΔG_{rxn} is the free energy of reaction, related to the equilibrium constant K_{eq} via $\Delta G_{rxn} = -k_B T \ln K_{eq}$. In the original Brønsted LFER for proton transfers in an acid catalysis,[108] the Brønsted coefficient α is a constant for single-step reactions so that there is a linear relation between the two free energies. By contrast, the Marcus relation—originating in electron-transfer theory,[45,46] extended to a range of reaction classes,[43,44,109,110] and based on two parabolic diabatic surfaces—predicts a quadratic equation, which yields

$$\alpha = \frac{1}{2}\left(1 + \frac{\Delta G_{rxn}}{4\Delta G_0^‡}\right) \tag{5.8}$$

where $\Delta G_0^‡$ is the so-called "intrinsic" barrier—the activation free energy for thermoneutral reactions.

Figure 14a displays two plots, the more curved (C1) for the complete decomposition to stable product states and the less curved (C2) for dissociation to an intimate ion pair (i.e., $r \lesssim 3.5$ Å). The first point of importance is that α is not at all a constant. For C1, α varies from 0.08 for a highly polar solvent ($\epsilon_0 \approx 80$) to 0.45 for a weakly polar solvent ($\epsilon_0 \approx 2.7$); α ranges from 0.18 to 0.45 for the curve C2. By assuming a linear interpolation, Leffler[111] pointed out that α measures the transition-state character; if α is close to 0, then the transition state is reactant-like; $\alpha \approx 1$ corresponds to a product-like transition state. Our calculated tendency for the α coefficients for both curves in fact does agree with the transition-state ionic character *trend*, i.e., more reactant-like (less ionic) transition state for a more polar solvent [Figure 8b]. This is clearly illustrated in Figure 14b, by the strong correlation between α and the transition-state ionic character.

Thus in principle, the α variation with solvent polarity, if determined with sufficient accuracy, can provide a possible experimental test for the transition-state ionic character trend predicted here.[112] This trend is at variance with the suggestion[20a] that, for

(106) To test the generality of the solvent polarity trends of the transition-state structure and the activation free energy established in section 5A and 5B, we have studied numerically two different cases by varying the electronic coupling $\beta(r)$. In the first case, the coupling is varied by changing D_0 in the pure covalent curve $\mathcal{H}_{11}^0(r)$ [eq 4.2] by ±5 kcal/mol with the ionic curve $\mathcal{H}_{22}^0(r)$ [eq 4.1] and the true *t*-BuCl gas-phase ground state $E_g(r)$ [eq 4.3] fixed.[77] In the second case, $\beta(r)$ is scaled by multiplying the actual coupling by some constant while the diabatic curves $V_C^0(r)$ and $V_I^0(r)$ remain fixed. (The new scaled coupling, together with $V_C^0(r)$ and $V_I^0(r)$, no longer yields the true gas-phase ground state in eq 4.3. Nonetheless, this exercise is useful in assessing the electronic coupling effect on the transition state and $\Delta G^‡$.) In both cases, an enhanced coupling (by reduction of D_0 in the first case[77] and by scaling up of $\beta(r)$ in the second case) yields a more ionic and less tight transition state for any given solvent polarity C. Howeve, the general tendencies for $c_I^{‡2}$ and $r^‡$ (i.e., less ionic—but always more than 50% ionic—and more tight transition state with increasing C) and for $\Delta G^‡$ remain intact for both cases. In particular, the electronic coupling reduction of $\Delta G^‡$ increases with growing solvent polarity C, while the transition-state solvation stabilization decreases. This indicates that the general trends we observed in the text are rather insensitive to the detailed parameters in the vacuum Hamiltonian once the general qualitative features for the diabatic curves and the electronic coupling remain the same. This strongly suggests that our conclusions in section 5 are robust. Further, we have determined that the same qualitative trends *also* follow in either of the BO or SC limiting regimes [cf. section 3A].

(107) A situation somewhat similar to this occurs in the solvolysis of triarylmethyl chloride. Due to a considerable charge delocalization in the aryl groups of the carbocation, there is significant solvent destabilization of the triarylmethyl cation compared to alkyl cations. See: Mason, S. F. *J. Chem. Soc. (London)* **1958**, 808.

(108) Brønsted, J. N.; Pedersen, K. *Z. Phys. Chem.* **1924**, *108*, 185.
(109) Marcus, R. A. *J. Phys. Chem.* **1968**, *72*, 891.
(110) Arnaut, L. G.; Formosinho, S. J. *J. Phys. Chem.* **1988**, *92*, 685.
(111) Leffler, J. E. *Science* **1953**, *117*, 340.

reactions describable in terms of two VB states, the Brønsted coefficient will not be correlated with the charge development in the transition state.

However, we add a cautionary remark. The α coefficient should be interpreted as a *relative*, rather than absolute, scale. From the above analysis, α is less than $^1/_2$ for $\epsilon_0 \gtrsim 2.7$, which translates to a more reactant-like than product-like transition state on an absolute scale—this contradicts the calculated absolute transition-state ionic character, which is always more than 50% ionic in this polarity range [Figure 8b].[113] We can find a further justification for the relative scale interpretation from Pauling's bond order[114] n defined as $r - r_{eq} = -0.26 \ln n$, where r and r_{eq} are bond lengths under consideration and at equilibrium, respectively. For $2.7 \lesssim \epsilon_0 \lesssim 80$ ($\epsilon_\infty = 2$), the transition-state bond order falls in the range $0.04 \lesssim n \lesssim 0.08$. Since $n = 1$ for the reactant state, this analysis would describe the transition state as more product-like. It is thus difficult to correlate α to the transition-state ionic character or geometry (or equivalently, bond order) on an absolute scale, although all of these show the same consistent *trend*, i.e., the more polar the solvent is, the more reactant-like and less product-like is the transition state.

Finally, to separate the kinetic and thermodynamic effects, the first derivative of α is usually employed to calculate the intrinsic barrier $\Delta G_0^\ddagger$. From the Marcus relation eq 5.8, one finds

$$\frac{d\alpha}{d\Delta G_{rxn}} = \frac{1}{8\Delta G_0^\ddagger} \tag{5.9}$$

which is potentially an account of the observed variation of α. The numerical results for $\Delta G_0^\ddagger$ obtained from eq 5.9 and 9 and 12 kcal/mol for C1 and C2, respectively. If eq 5.8 were valid for S_N1 ionizations, then $\Delta G_0^\ddagger$ could also be evaluated as a y-intercept from Figure 14a. The result *is* roughly 28 kcal/mol for both curves C1 and C2, which is far greater than the estimates just given. This inconsistency shows that the Marcus eq 5.8 is not applicable to the current S_N1 ionization processes. We can advance several reasons for this: (a) the two diabatic curves are far from parabolic, (b) the electronic coupling is strong and strongly depends upon r, and (c) the solvent stabilization is not constant but rather changes with r.

ii. **Activation and Transfer Free Energy Relation.** We can consider another possible and different type of LFER. From eq 5.1 we can obtain an approximate relation between the activation free energy $\Delta G^\ddagger$ and the solvent reorganization free energy at the transition state

$$-\frac{d\Delta G^\ddagger}{d\Delta G_r(r^\ddagger)} \sim s^{\ddagger 2} \simeq c_1^{\ddagger 4} \tag{5.10}$$

In deriving this, we have divided eq 5.1 by $M_s(r^\ddagger)$, approximated $r^\ddagger$ as a constant when the polarity factor C is varied and invoked the feature that the reactant free energy—being to a high degree of approximation that of the covalent state—is essentially independent of solvent polarity. The simplicity of eq 5.10 giving the transition-state charge distribution must be counted as rather surprising considering the fact that the two-state model is quantum mechanical in nature with a large covalent ionic electronic coupling of ~13–18 kcal/mol near the transition state—features shown in sections 4B, 5A, and 5B to be crucial in determining the activation free energy and transition-state ionic character. We have verified numerically that it is accurate to better than 5% over the polarity range $3 \lesssim \epsilon_0 \lesssim 80$.

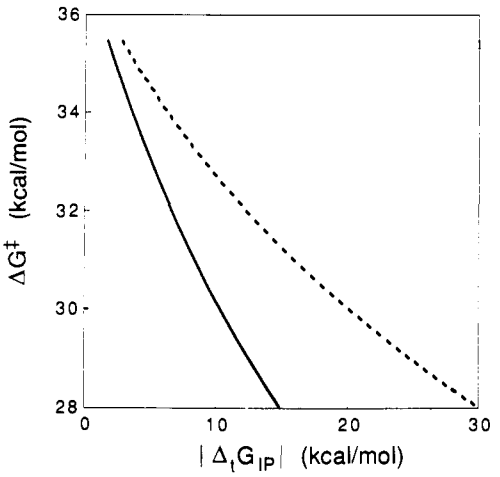

Figure 15. $\Delta G^\ddagger - \Delta_t G_{IP}(r^\ddagger)$ plot. For (—) the transfer free energy with the transition-state separation $r^\ddagger$ is used. The free energy of transfer employed in (···) is that of an intimate ion pair ($r \approx 3.5$ Å). Since $|\Delta_t G_{IP}|$ for the latter is significantly larger than that with the transition-state separation, the slope for the latter is about one-half of that for the former.

We pause to consider a useful physical meaning to be attached to $\Delta G_r(r^\ddagger)$ from a perspective different from the solvent reorganization aspect given in section 2. From eqs 3.10, 3.11, and 3.13, the equilibrium free energy for an ion pair R^+X^- (i.e., $s = c_1^2 = 1$) with separation r is given by

$$G_{IP}^{eq}(r) = G(r,s=1) = V_1(r,s=1) - k_B T \ln [r/r_0]^2 + \Delta G_r(r)$$

$$= V_1^0(r) - k_B T \ln [r/r_0]^2 - \Delta G_r^{el}(r) - \Delta G_r(r) \tag{5.11}$$

Now we consider the free energy of transfer for this ion pair from a nonpolar to a polar solvent. If we assume that the ion pair separation r does *not* change with solvent polarity, the free energy of transfer $\Delta_t G_{IP}(r)$ then becomes

$$\Delta_t G_{IP}(r) \equiv G_{IP}^{eq}(r)(\text{polar solvent}) - G_{IP}^{eq}(r)(\text{nonpolar solvent}) = -\Delta G_r(r) \tag{5.12}$$

The solvent reorganization free energy is therefore the magnitude of the free energy of transfer for an ion pair from a nonpolar to a polar solvent.[18b] Thus $\Delta G_r(r^\ddagger)$ is (up to a sign) the free energy of transfer for an (unstable) ion pair at the t-BuCl transition-state separation $r^\ddagger$. We also note parenthetically that $\Delta G_r(r^\ddagger)$ is, in a general way, similar to experimental solvent polarity factors such as the Kosower Z value[104,115] and $E_T(30)$,[80] defined as the Franck–Condon spectroscopic transition energy between the ionic ground and the covalent excited states of reference molecules in a solvent.[116,117]

Returning to our main thread, eq 5.10 determines the ionic character of the transition state $c_1^{\ddagger 2}$; if one can evaluate or estimate $\Delta G_r(r^\ddagger) = -\Delta_t G_{IP}(r^\ddagger)$ by certain means, the ionic character can

(112) By using the experimental data compiled in ref 11a and by assuming that tetramethylammonium chloride is a reasonable model for t-BuCl ion pair in solution, we have examined the α variation with activation free energy in various aprotic solvents. The result agrees qualitatively with the α trend expected from Figure 14, though it is considerably weaker than the predicted α trend. However, considering the experimental data uncertainties and the crucial assumption made for the t-BuCl ion pair, α determined from currently available experimental data cannot be said to provide convincing evidence for the predicted transition-state ionic character trend. Experimental studies with a much improved accuracy are needed.

(113) By correlating rate and equilibrium constants for various reactants in a fixed polar solvent (rather than varying solvent polarity with fixed reactants), one can obtain a different Brønsted coefficient α, rather close to 1 (see ref 8d and also: Rudakov, E. S.; Kozhevnikov, I. V.; Zamashchikov, V. V. *Russ. Chem. Rev.* **1974**, *43*, 305).

(114) Pauling, L. *J. Am. Chem. Soc.* **1947**, *69*, 542.

(115) Kosower, E. M. *J. Am. Chem. Soc.* **1958**, *80*, 3253.

(116) van der Zwan, G.; Hynes, J. T. *J. Phys. Chem.* **1985**, *89*, 4181.

(117) One major difference, though, is that these experimental factors include the contributions from both the solvent electronic and orientational polarizations, while only $\bar{P}_{or}$ contributes to $\Delta G_r(r^\ddagger)$. (However, if the reference molecule fluoresces and if its electronic structure does not change much along the solvent coordinate, the red-shift of the steady-state emission line with respect to the absorption line is, to a good approximation, $2\Delta G_r$; the solvent electronic contributions to absorption and emission lines cancel out in the red-shift.[104,115]) Thus $\Delta G_r(r^\ddagger)$ is proportional to the Pekar factor C; it is a very convenient *free energy* scale, measuring the solvent polarity just like the Kosower Z value and $E_T(30)$. However, $\Delta G_r(r^\ddagger)$ has a thermodynamical interpretation (free energy of transfer) rather than a spectroscopic aspect. Nonetheless, within certain plausible approximations, the difference of Z values between a given solvent and a highly nonpolar one is equal to ΔG_r [cf. eq 3.19 of ref 116].

then be obtained as the square root of the slope for a $\Delta G^{\ddagger} - \Delta_t G_{IP}(r^{\ddagger})$ plot, illustrated in Figure 15. The approximate linear relationship there denotes that the transition-state ionic character $c_1^{\ddagger 2}$ depends only weakly on the solvent polarity. The linearity is actually analogous—although in somewhat disguised form—to the experimentally observed[115] linear relation of the Grunwald–Winstein[3a] solvent ionizing power Y parameter and the solvatochromic Kosower Z parameter.[104,115] This feature is important, given our novel interpretation and predictions for the transition-state ionic character and origin of the solvent polarity dependence of $\Delta G^{\ddagger}$. We stress that eq 5.10 is valid only if $r^{\ddagger}$ depends very weakly on the solvent polarity (and here it does).

There have been extensive experimental efforts to determine the transition-state ionic character for *t*-BuCl.[11,12,97] When $\Delta G^{\ddagger}$ is plotted against the free energy of transfer for the ion pair $Me_4N^+Cl^-$ from a reference solvent to various solvents, the slope has been interpreted by Abraham and co-workers as the degree of ionic character (here $c_1^{\ddagger 2}$) at the transition state.[11,97] In view of our analysis [eq 5.12], an implicit important assumption made there is that the ion pair separation for $Me_4N^+Cl^-$ and $r^{\ddagger}$ for *t*-BuCl are the *same*. This assumption is necessary to equate the free energy of transfer for $Me_4N^+Cl^-$ with $\Delta G_t(r^{\ddagger}) = -\Delta_t G_{IP}(r^{\ddagger})$ for *t*-BuCl in our language. If the transition state for *t*-BuCl were 100% ionic, then the slope between $\Delta G^{\ddagger}$ and the free energy of transfer would be unity; if completely covalent, it would vanish.[118] Between these two extremes, a simple linear relationship between the slope and the transition-state ionic character is then posited.[11] Thus, for example, a slope of 0.7 is translated to a 70% ionic transition state for *t*-BuCl.

According to our two-state quantum theory, however, this *basic* interpretation—slope = ionic character—is fundamentally incorrect. We first note that since the variation in $r^{\ddagger}$ is minor with the solvent polarity, the change in $\Delta G_t(r^{\ddagger})$ with the solvent polarity that we predict is the *same* as that in the free energy of transfer for the ion pair according to the observations made above [cf. eq 5.12]. The transition-state ionic character is then the *square root* of the slope, not the slope itself, in the $\Delta G^{\ddagger}$-free energy of transfer plot[119] according to eq 5.10. Since the slope magnitude is always less than one, the square root of the slope is larger than the slope. We would therefore reinterpret the experimental data, to conclude that $c_1^{\ddagger 2}$ is larger and thus the transition state is more ionic in character than originally estimated in the literature.[11] For instance, if we take 0.5 as the slope for *tert*-butyl chloride in weakly polar and nonpolar aprotic solvents,[11a,b] the actual ionic character at the transition state would be about 0.7, which is a 40% increase of the original estimate based on a slope analysis.[121,123]

It is also useful to relate and compare our results to the transition-state electric dipole moment $\mu^{\ddagger}$ obtained in the classical Kirkwood picture[120] for point dipole solvation applied to the S_N1 problem.[11c,12,16a] The activation free energy and $\mu^{\ddagger}$ in this description are related by

$$\Delta G^{\ddagger} = \Delta G_0^{\ddagger} - \frac{\epsilon_0 - 1}{2\epsilon_0 + 1}\frac{\mu^{\ddagger 2}}{a^{\ddagger 3}} \qquad (5.13)$$

where $\Delta G_0^{\ddagger}$ denotes the activation free energy independent of $\mu^{\ddagger}$, and $a^{\ddagger}$ is the cavity size for the transition-state complex. The solvation free energy $\Delta G^{K}_{\ddagger,solv}$ in this description is given by

$$\Delta G^{K}_{\ddagger,solv} = -\frac{\epsilon_0 - 1}{2\epsilon_0 + 1}\frac{\mu^{\ddagger 2}}{a^{\ddagger 3}} \qquad (5.14)$$

This Kirkwood description is the most widely used and accepted picture in explaining the activation free energy change with solvent polarity due to nonspecific solvation. The simple classical dipole description posits that only the solvation stabilization via electrostatic interactions contributes to the activation free energy change with solvent polarity and thus the effect of any change in the electronic coupling is totally absent.

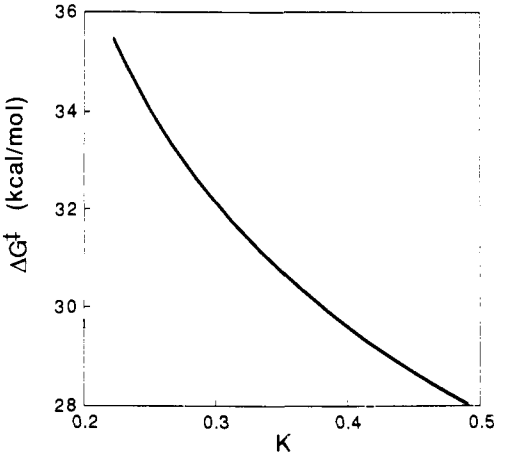

Figure 16. $\Delta G^{\ddagger}$ vs the Kirkwood polarity factor $K = (\epsilon_0 - 1)/(2\epsilon_0 + 1)$.

Since the proportionality constant in eq 5.13 is $\mu^{\ddagger 2}/a^{\ddagger 3}$ when $\Delta G^{\ddagger}$ is plotted against the Kirkwood polarity factor $(\epsilon_0 - 1)/(2\epsilon_0 + 1)$, one can determine the transition-state dipole moment $\mu^{\ddagger}$ once the cavity size $a^{\ddagger}$ is known. By following ref 11c, we can determine the cavity size by the relation $a^{\ddagger 3} = (3V/4\pi N)$ with the molar volume $V = 116$ cm^3 for *t*-BuCl. When our $\Delta G^{\ddagger}$ is plotted against the Kirkwood polarity factor $K = (\epsilon_0 - 1)/(2\epsilon_0 + 1)$, a rather linear relationship is obtained [Figure 16]. Since K is almost linearly related to C for $\epsilon_0 \gtrsim 3$, this linearity in Figure 16 is to be expected from Figure 15 (and also from Figure 13). From the slope with $a^{\ddagger} = 3.58$ Å, we find that $\mu^{\ddagger} \approx 8.2$ Debye, which is in good agreement with other values quoted in the literature.[11c] For comparison, from the relation $\mu^{\ddagger} = er^{\ddagger}c_1^{\ddagger 2}$, our theory also predicts directly from the calculated ionic character $c_1^{\ddagger 2}$ that $\mu^{\ddagger} \approx 7.2 - 9.6$ Debye but in contrast reflects a change in $\mu^{\ddagger}$ with solvent polarity. In addition, both the electronic coupling and the solvation are properly taken into account in our theory in contrast to the classical Kirkwood description. In particular, while the overall trend of $\Delta G^{\ddagger}$ with solvent polarity is correctly given by $\Delta G^{K}_{\ddagger,solv}$, we have seen in section 5B that the $\Delta G^{\ddagger}$ variation is instead due to the trend in the electronic coupling, which here is (at best) concealed in $\Delta G_0^{\ddagger}$: the actual transition-state solvation free energy $\Delta G^{eq}_{\ddagger,solv}$ goes in the *opposite* direction to $\Delta G^{\ddagger}$ (and $\Delta G^{K}_{\ddagger,solv}$). The classical description misses completely the transition-state structure change in eq 5.5.

6. Concluding Remarks

In this paper, we have investigated S_N1 ionic dissociation reactions for *t*-BuCl in solvents of different polarity by employing a quantum two-state Hamiltonian combined with a dielectric continuum description for the solvent. The free energy surface obtained in terms of the solvent coordinate s and the internuclear separation r has enabled us to analyze the structure of the transition state relevant to the ionization reaction and the reaction free energetics.

(118) When the free energy of transfer for a nonelectrolyte is plotted against that for $Me_4N^+Cl^-$, it yields a smooth curve rather than a straight line with zero slope.[11]

(119) This also qualitatively agrees—rather remarkably in view of the complexities which govern the transition-state charge distribution—with the result if a simple classical dipole description[120] is simply invoked.[12,16a,43]

(120) Kirkwood, J. G. *J. Chem. Phys.* **1934**, *2*, 351.

(121) It is also worthwhile to assess a possible error involved in the assumption that the $Me_4N^+Cl^-$ ion pair separation is $r^{\ddagger}$, which is about 2.5 Å. If we assume that the ion pair separation is instead around 3.5 Å and that $\Delta G_t(r)$ increases linearly with r in this region, we estimate approximately

$$\Delta G_t(r = 3.5\text{ Å}) \simeq 1.4\Delta G_t(r = 2.5\text{ Å})$$

The experimentally observed slope would then be about 40% smaller than the value which should be used in calculating the transition-state ionic character [cf. Figure 15]. Thus, correlating $\Delta G^{\ddagger}$ with $\Delta_t G_{IP}$ requires considerable caution.[122]

(122) We reemphasize that the weak dependence of $r^{\ddagger}$ upon the solvent polarity makes our approximate correlation eq 5.10 valid. If $r^{\ddagger}$ varies considerably with solvent polarity, we no longer find any simple relation between $\Delta G^{\ddagger}$ and $\Delta_t G_{IP}$, even when the ion pair separation is the same as $r^{\ddagger}$.

(123) In view of the tendency[33] for solvents described molecularly to act as if they were less polar than their continuum description would portray them, the transition-state character is likely more ionic than estimated from a continuum characterization.

Our theoretical analysis predicts results which contradict several traditional notions for the S_N1 ionization process, including the Hughes–Ingold transition-state solvation stabilization rationale for decreasing activation barriers with increasing solvent polarity. Most notable of these predictions are as follows: (a) the transition state is less polar and more tight as the solvent polarity increases; (b) the dominant source of the trend that the activation free energy drops as the solvent becomes more polar is the variation of the electronic coupling between the covalent and ionic states; and (c) the transition-state solvation free energy stabilization diminishes for increasing solvent polarity. We have presented analytical and qualitative arguments which both confirm the observed numerical results and indicate that they can be comprehended in terms of the competition between electronic coupling—which favors a delocalized 50% ionic transition state—and solvation—which favors a localized, purely ionic transition state. It is important to stress that, in addition to these markedly nonconventional predictions, our theory also predicts various experimentally observed trends, e.g., approximately linear dependence of the activation free energy (a) on transfer free energies (in analogy to a linear relation[104,115] between the Grunwald–Winstein[3a] solvent ionizing power Y parameter and the solvatochromic Kosower Z polarity scale[104,115]) and (b) on the Kirkwood polarity factor.[11c,12] It is essential to note also that these approximately linear relationships do not themselves give any explicit, qualitative indication of the nonconventional transition-state structure and activation free energy source that we have found. It seems to us that this feature as well as the lack of any prior analysis along the lines of our present effort has contributed to the delay in the finding of the novel S_N1 ionization transition-state structure and free energetic aspects predicted here. We have indicated that the solvent polarity dependence of a Brønsted coefficient [section 5C.i] could serve as an experimental probe of our predictions.

We have also found, in contradiction to frequently employed assumptions,[11] that the transition-state ionic character is related to the square root of the slope (and not the slope) of an activation free energy–transfer free energy plot for the S_N1 ionization process.[124]

The solvent polarity has been described via a dielectric continuum depiction. A more molecular description of the solvent is clearly desirable, and a microscopic version of the present theory is under construction. We anticipate that the qualitative trends that we have found will be preserved but that quantitative aspects will change to some degree (see, e.g., ref 123). The largest changes should arise when there are specific solvation effects. For example, for hydroxylic solvents such as water and the alcohols, the specific electrophilic solvation of the t-BuCl ionic state via hydrogen bonding can play a significant role in determining the activation

$$Bu^+Cl^-\cdots H^{+\delta}O^{-\delta}R$$

free energy.[11,12,15,16a] The net effect of the hydrogen bonding in the simplest language is an additional stabilization of the ionic curve,[126] beyond simple solvent polarity expectations; this should result in an earlier diabatic curve crossing, yielding a lower activation barrier than in a nonhydroxylic solvent with the same solvent polarity, i.e., with the same dielectric constant. By analogy to our general analysis of transition-state character trend with solvent polarity, we can conclude from this observation that if the solvent polarity C is the same for say any two hydroxylic solvents, we expect that the higher is the hydrogen bonding ability of the solvent, the less ionic and more tight is the transition state. One important step toward a more microscopic description is the first molecular dynamics computer simulation of the dynamics of an S_N1 ionization, roughly based on t-BuCl in water, by Keirstead et al.[83]—based largely on a simplified version of the formulation here and in part 2. The solute model employed[83] shares some similarities with, but also has a number of differences from, the t-BuCl model used here; the reader is referred to ref 83 for the details.

Finally, the current formulation for S_N1 ionizations in the two-dimensional reaction coordinate system (r, s) can be applied to examples other than t-BuCl[127,128] and can be adapted to describe other unimolecular charge-transfer processes, e.g., proton transfer—especially acid dissociation,[55] hydride transfer,[129] and reactions in twisted intramolecular charge-transfer complexes[130] as well as, e.g., photoionizations[131] and S_N2 reactions.[132] In all these problems, the transition-state free energy, structure, and charge distribution should be determined by the competition between solvation and electronic coupling.

Acknowledgment. This work was supported in part by NSF Grant CHE88-07852 and NIH Grant RO1 GM 41332. We thank Dr. W. Keirstead and Prof. K. R. Wilson for useful discussions concerning the vacuum S_N1 potentials, Prof. S. S. Shaik for a fruitful correspondence, and Jeff Mathis for helpful discussions.

Appendix. Transition-State Analysis

We begin the analysis proper by invoking the equilibrium relation eq 3.13, to obtain from eqs 3.9 and 3.11, the transition-state (TS) condition

(124) At this point, we address an experimental data activation-transfer free energy $\Delta G^* - \Delta_t G_{IP}$ plot for t-BuCl decomposition presented by Abraham and co-workers,[11] where the slope for less polar aprotic solvents is less than for hydroxylic solvents. But by our eq 5.10 this plot would indicate that the transition-state (TS) ionic character is less for the aprotic solvents. This seemingly disagrees with our conclusion that the ionic character should be more polar in the less polar aprotic, compared to the more highly polar, hydroxylic solvents. (This difficulty is not resolved by appeal to our slope–square root ionic character relation eq 5.10, as opposed to a linear slope–ionic character relation;[11] this is a quantitative but not a qualitative difference.) The most likely source of the disagreement is that the cited $\Delta G^* - \Delta_t G_{IP}$ plot[11] does *not* refer to S_N1 ionization in each of the solvent classes (a point appreciated by the authors of ref 11c). In particular, the t-BuCl decomposition mode in the hydroxylic solvents is S_N1, but in the aprotic solvents, it is instead under the experimental conditions the unimolecular E1 elimination noted in the Introduction. This difference can itself lead to a slope change *unrelated* to the solvent polarity trends we have discussed. In particular, internal solvation of the TS via an induced dipole moment in a C–H bond in a methyl group of t-Bu cation[11c,12,16a,39] would shield the t-BuCl charge distribution; this would decrease the apparent dipole moment of the C–Cl bond vis-ă-vis the solute–solvent electrostatic interactions. The solvation effect at the TS would then become less sensitive to solvent polarity, while $\Delta_t G_{IP}$ (for an ion pair $Me_4N^+Cl^-$) measured in a separate experiment would not be affected by this internal solvation. As a result, the actual change $\Delta\Delta G^*$ for different solvents would be reduced compared to our model calculations while the corresponding change $\Delta\Delta_t G_{IP}$ remains the same; this would result in a smaller slope for E1 reactions than predicted in our model calculations (which appropriately ignore any such internal solvation for the S_N1 process).[125]

(125) This, however, does not seem to agree on the surface with the experimental results of Koppel and Palm,[12a] who measured the t-BuCl decomposition rate k for a mixture of aprotic solvents with alcohols at high temperature and then linearly extrapolated $-\ln k$ to zero alcoholic concentration. Their results indicate that $\Delta\Delta G^*$ obtained via linear extrapolation is smaller than that from the E1 reactions, although by $\lesssim$1 kcal/mol. However, in view of section 3 of part 2 and the uncertain transition-state character[11c,12,16a,39] of the E1 mechanism, it is unclear if differences of this magnitude are significant. The linear extrapolation of $-\ln k$ by Koppel and Palm can be another source of uncertainty, since a linear dependence of k (rather than $-\ln k$) on the alcoholic concentration has been observed in nitromethane–alcohol mixtures.[1e]

(126) One can implement the solvent stabilization due to hydrogen bonding in a very approximate model calculation (in an analogous way to $M_s(r)$ in eq 2.10), but we will not pursue this here.

(127) Application to the reverse, cation–anion recombination reaction class[10,21b] could also be undertaken. In particular, this might provide some more fundamental justification for the parametric equation of Shaik[21b] for the reaction barrier. (We thank Prof. S. S. Shaik for correspondence on this point.)

(128) Mathis, J. R. et al. in ref 103.

(129) After the submission of this paper, we became aware of Tapia O.; Andres, J.; Aullo, J. M.; Cardenas, R. *J. Mol. Struct.* **1988**, *167*, 395 in which is studied, via computation, the hydride transfer $CP^+\cdots H_3CO^- \rightarrow CPH + H_2CO$ with CP = cyclopentadienyl. These authors find that increasing reaction field stabilization (modeled to be relevant to a protein) of the ionic reactants leads to transition state barrier and ionic character trends consistent with the Hammond postulate and which lend support to the present work.

(130) Barbara, P. F.; Kang, T. J.; Jarzeba, W.; Fonseca, T. In *Perspectives in Photosynthesis*; Jortner, J., Pullman, B., Eds.; Kluwer: Dordrecht, 1990. Barbara, P. F.; Jarzeba, W. *Adv. Photochem.* **1990**, *15*, 1.

(131) See, for example: Goodman, J. L.; Peters, K. S. *J. Am. Chem. Soc.* **1985**, *107*, 6459. Spears, K. G.; Gray, T. H.; Huang, D.-Y. *J. Phys. Chem.* **1986**, *90*, 779.

(132) See, e.g., Gertner, B. J.; Wilson, K. R.; Hynes, J. T. *J. Chem. Phys.* **1989**, *90*, 3537, and references therein.

$$\left.\frac{\partial G}{\partial r}\right|_* = G_C^{eq\prime} + (G_I^{eq\prime} - G_C^{eq\prime})s^* - 2\beta'[s^*(1-s^*)]^{1/2}\left[1 - \frac{\Delta G_r^{el}}{2\hbar\omega_{el}}(1-f^*)^2\right] + \Delta G'_r s^*(1-s^*) + \Delta G_r^{el\prime} s^*(1-s^*)f^* - \frac{2k_BT}{r^*} \approx G_C^{eq\prime} + (G_I^{eq\prime} - G_C^{eq\prime})s^* - 2\tilde{\beta}'[s^*(1-s^*)]^{1/2} + \Delta G'_r s^*(1-s^*) + \Delta G_r^{el\prime} s^*(1-s^*)f^* - \frac{2k_BT}{r^*} = 0 \quad (A.1)$$

where $\tilde{\beta} \equiv \beta[1 - (\Delta G_r^{el}/2\hbar\omega_{el})]$ and where G_C^{eq}, G_I^{eq} are, respectively, the equilibrium free energies for the solvent-equilibrated covalent and ionic states [eqs 2.11 and 2.12], and $'$ denotes an ordinary r derivative. The last approximate equality is valid to the linear order in ρ [cf. eqs 3.1 and 3.4]. All the r derivatives are evaluated at $r = r^*$. Since eq A.1 is a formal relation between r^* and s^*, it needs to be supplemented by eq 3.9 to explicitly determine r^* and s^*.

To examine how the TS structure varies with solvent polarity, we first rewrite eq A.1 as

$$G_C^{eq\prime} - [G_C^{eq\prime} - G_I^{eq\prime}]\left(\frac{1}{2} + \delta\right) - \tilde{\beta}'[1 - 4\delta^2]^{1/2} + \frac{1}{4}\Delta G'_r(1 - 4\delta^2) - \frac{2k_BT}{r^*} = 0 \quad (A.2)$$

where δ measures the TS deviation from the equal mixture of covalent and ionic states

$$c_I^{*2} = s^* \equiv \frac{1}{2} + \delta \quad (A.3)$$

Since δ is rather small ($\delta^2 \ll 1$ for a wide polarity range), we neglect terms of order δ^2 or higher in eq A.2 to obtain

$$\delta = \frac{G_{1/2}'}{G_C^{eq\prime} - G_I^{eq\prime}}$$

$$G_{1/2} \equiv \frac{1}{2}(G_C^{eq} + G_I^{eq}) + \frac{1}{4}\Delta G_r - \tilde{\beta} - k_BT \ln [r/r_0]^2 \quad (A.4)$$

where $G_{1/2}$ is the free energy eq 3.11 with $s = c_I^2 = {}^1/_2$, i.e., a hypothetical free energy quantity that varies with r in the presence of a fixed solvent coordinate $s = {}^1/_2$ and a fixed t-BuCl electronic structure $c_C^2 = c_I^2 = {}^1/_2$. (It is also the TS contribution to the approximate eq 2.21 in the $\rho = 0$ limit.) Note that at the diabatic crossing point $r = r_{cr}$, $G_{1/2}$ becomes the equilibrium free energy $G_{cr}^{eq} = G(r = r_{cr}, s = {}^1/_2)$ with an equal mixture of the ionic and covalent states. By noticing that (a) G_I^{eq} decreases monotonically, i.e., $G_I^{eq\prime} < 0$ between the reactant and product states, while G_C^{eq} is a monotonically growing function [Figure 10] so that $G_C^{eq\prime} - G_I^{eq\prime} > 0$, (b) the electronic coupling gradient β' is a negative number of a large magnitude for $r \lesssim 3$ Å [Figure 4], and (c) the reorganization free energy in a polar solvent increases progressively with r so that $\Delta G'_r > 0$, we conclude that $G_{1/2}' > 0$ unless the equilibrated ionic term $G_I^{eq\prime}$ in the numerator should dominate the other terms, which seems a remote possibility. Thus δ is positive (i.e., $c_I^{*2} > 0.5$); the TS is usually, if not always, more, rather than less, than 50% ionic.[103] This is consistent with our numerical calculations [Figure 8b].

We pause to note that if the electronic coupling $\beta(r)$ were a constant ($\beta' = 0$), then $G_{1/2}' < 0$ so that δ in eq A.4 would be negative; the TS would be less than 50% ionic. (With $\beta \approx 15$ kcal/mol, a saddle-point analysis on the full two-dimensional free energy surface yields $s^* \approx 0.3$.) This shift toward a more covalent TS with constant $\beta(r)$ is due to the influence of diabatic curve-skewing,[19b,21a] i.e., the magnitude of the slope for $G_I^{eq}(r)$ is larger than that for $G_C^{eq}(r)$ [cf. Figures 9 and 10]. For t-BuCl ionization in solution, this curve-skewing is completely opposed and dominated by the actual r-dependence of the electronic coupling $\beta(r)$, which shifts the TS toward the more ionic side. As discussed below, however, the change in the curve-skewing effect with the solvent polarity C is important for the TS ionic character trend.

In order to explicitly determine the TS, we combine eq 3.9 with the equilibrium condition eq 3.13 to obtain a variation of a nonlinear Schrödinger equation satisfied by an equilibrium solvation state[133]

$$-4\tilde{\beta}\delta - [G_I^{eq} - G_C^{eq}](1 - 4\delta^2)^{1/2} + 2\delta\Delta G_r(1 - 4\delta^2)^{1/2} = 0 \quad (A.5)$$

We now solve this nonlinear equation perturbatively in δ. In the zeroth order, $G_I^{eq} = G_C^{eq}$, which is satisfied at the diabatic crossing point r_{cr}. This in fact forces us to expand the r coordinate at the crossing point; thus a perturbation expansion in $\delta r \equiv r^* - r_{cr}$ is also required. In other words, a consistent perturbation solution for eq A.5 is such that we need to expand both s^* and r^* at $s^* = {}^1/_2$ and $r^* = r_{cr}$. This kind of constraint is to be expected since a reference point for the perturbation expansions (here $r = r_{cr}$ and $s = {}^1/_2$) also needs to lie on the free energy surface.

In the linear order for both δ and δr, we find from eq A.5

$$\delta r = \frac{2[2\tilde{\beta} - \Delta G_r]}{G_C^{eq\prime} - G_I^{eq\prime}}\delta \quad (A.6)$$

All derivatives in eq A.6 are evaluated at $r = r_{cr}$ in contrast to eqs A.2 and A.4. Since δ is usually positive and $G_C^{eq\prime} - G_I^{eq\prime} > 0$ as pointed out above, the sign of δr depends on the relative magnitudes of the electronic coupling β and the reorganization free energy ΔG_r. If the solvation effect were to dominate the quantum coupling, then the numerator becomes negative and so does δr; the actual TS would be tighter than the crossing point prediction r_{cr}.[128] But in the strong coupling limit, β dominates and thus $r^* > r_{cr}$. As to the shift magnitude, for our t-BuCl model ($3 \lesssim \epsilon_0 \lesssim 80$), a large coupling (15–18 kcal/mol) in the TS region [Figure 4] is opposed by the solvation free energy ($\Delta G_r \approx 5$–15 kcal/mol), while the slope difference range is 100–150 kcal/mol/Å; as a result, the magnitude of the proportionality constant in front of δ in eq A.6 is ~0.25–0.35 Å; the TS separation r^* is thus only slightly larger than r_{cr}. This is just what we have observed in the numerical calculations in Figure 10.

To see how r^* changes with solvent polarity in the strong electronic coupling limit, we again examine a perturbation solution for r^* around the diabatic crossing point $r = r_{cr}$. Since that point is given by $G_I^{eq}(r_{cr}) - G_C^{eq}(r_{cr}) = 0$, we differentiate this equation with respect to C to obtain [cf. eqs 2.12 and 2.13]

$$\frac{dr_{cr}}{dC} = \left(1 - \frac{1}{\epsilon_0}\right)^{-1}\frac{\Delta G_{I,solv}^{eq}}{G_C^{eq\prime} - G_I^{eq\prime}} = -\left(\frac{1}{\epsilon_\infty} - \frac{1}{\epsilon_0}\right)^{-1}\frac{\Delta G_r}{G_C^{eq\prime} - G_I^{eq\prime}} < 0 \quad (A.7)$$

As we now expect, r_{cr} decreases (i.e., there is an earlier diabatic curve crossing) with increasing solvent polarity. By taking the C derivative of eq A.6 and neglecting the small correction terms proportional to δr, we deduce that $dr^*/dC = dr_{cr}/dC + d\delta r/dC \approx 2s^* dr_{cr}/dC < 0$. Thus the TS is predicted to become tighter with increasing solvent polarity, as observed in Figure 8a.

Having established how r^* changes with the solvent polarity factor C, we now proceed to the TS charge distribution $s^* = c_I^{*2}$. Though this can be investigated analytically by differentiating eq A.4 with respect to C, we do here a rather qualitative analysis based on our numerical calculations. Both the numerator and denominator in δ, eq A.4, vary with solvent polarity. The main source of this is the change in the coupling derivative $\tilde{\beta}'$ and the equilibrated ionic curve slope $G_I^{eq\prime}$. For $3 \lesssim \epsilon_0 \lesssim 80$, the latter ranges −50 to −110 kcal/mol/Å, while the former changes from ≈−30 to ≈−45 kcal/mol/Å. (The other quantities remain relatively unchanged; $G_C^{eq\prime} \approx 45$–50 kcal/mol/Å and $\Delta G'_r/4 \approx 1$–3 kcal/mol/Å.) This is due to the fact that both derivatives $G_I^{eq\prime}$

(133) We remark that any equilibrium solvation state should satisfy eq A.5 with a minor redefinition for δ, i.e., $s_{eq} = {}^1/_2 + \delta$.[27] Since our main interest lies in the transition state, we will focus only on s^* here.

and β' (and not the functions themselves) are strongly increasing functions of r near the TS region, which can be easily seen by differentiating the relevant curves in Figure 4 (see also Figure 10). We can also infer from this that $G_I^{eq\prime}$ is a stronger function of r than is β' because the ionic potential is much more curved. With these observations, we now consider how δ behaves with the solvent polarity. With increasing C, both $G_I^{eq\prime}$ and β' decrease at the transition state, since $r^\ddagger$ diminishes as explained above. Therefore, the denominator $G_C^{eq\prime} - G_I^{eq\prime}$ of δ grows. The numerator behavior with C is not so apparent due to the opposing effects of $G_I^{eq\prime}$ and $-\beta'$. Howeve, since $G_I^{eq\prime}$ is a stronger function of r, $G_I^{eq\prime}/2 - \beta'$ decreases, and so does the numerator. As a result, δ diminishes with C. We thus conclude that the TS ionic character $c_I^{\ddagger 2}$ wanes with increasing solvent polarity.

Registry No. *t*-BuCl, 507-20-0; *t*-BuI, 558-17-8; $Me_4N^+Cl^-$, 75-57-0.

A Theoretical Model for S_N1 Ionic Dissociation in Solution. 2. Nonequilibrium Solvation Reaction Path and Reaction Rate

Hyung J. Kim† and James T. Hynes*

Contribution from the Department of Chemistry and Biochemistry, University of Colorado, Boulder, Colorado 80309-0215. *Received April 3, 1991*

Abstract: The theoretical formulation developed in the preceding article [Kim, H. J.; Hynes, J. T. *J. Am. Chem. Soc.*, preceding paper in this issue] is applied to determine the reaction path and rate constant for the S_N1 ionization process in solution RX $\rightarrow R^+ + X^-$, illustrated for *t*-BuCl. It is found that the intrinsic solution reaction path (SRP), which is the analogue of the familiar minimum energy path of gas-phase reaction studies, differs considerably from the conventionally assumed equilibrium solvation path (ESP). In particular, the SRP near the transition state lies mainly along the RX separation coordinate r. There is little motion in the solvent coordinate s; the solvent lags the solute nuclei motion and there is nonadiabatic nonequilibrium solvation. Near the reactant configuration RX, however, the critical motion initiating the reaction is that of the solvent, i.e., the solvent orientational polarization. The contrasts with activated electron transfer are also pointed out. The connection of the two-dimensional (r, s) free energy surface to the potential of mean force is made, particularly in connection with the ionization activation free energy, as is the connection to the conventional transition-state theory (TST) rate constant k^{TST}, which assumes equilibrium solvation. The deviation of the actual rate constant k from its TST approximation (the transmission coefficient $\kappa = k/k^{TST}$) due to nonequilibrium solvation is examined, via both linear and nonlinear variational transition state theory. Despite the pronounced anharmonicity of the (r, s) free energy surface arising from the electronic mixing of the covalent and ionic valence bond states, a simple harmonic nonadiabatic solvation analysis is found to be suitable. This analysis predicts progressively larger and more significant departures from equilibrium solvation TST with increasing solvent polarity.

1. Introduction

In the preceding article,[1] hereafter referred to as part 1, we have developed a theoretical formulation to describe the unimolecular S_N1 ionization process RX $\rightarrow R^+X^-$ in solution. Our focus there was on the reaction free energetics and the electronic structure of the transition state, features which we examined via an implementation of the theory for a model of *t*-BuCl ionization in a dielectric continuum solvent. In particular, the S_N1 solute electronic structure represented by its wave function Ψ was studied, in a simple two orthonormal valence bond state basis consisting of a covalent state $\psi_C[RX]$ and an ionic state $\psi_I[R^+X^-]$, via

$$\Psi(r,s) = c_C\psi_C[RX] + c_I\psi_I[R^+X^-] \qquad (1.1)$$

where the state coefficients c_C, c_I depend on both the RX nuclear separation coordinate r and the collective solvent coordinate s. (See section 2 and 4A of part 1 for details on this basis set.)

In the present article, we turn our attention to two different aspects of the ionization, namely, the reaction path and the reaction rate constant. For this purpose, we again exploit the theoretical determination of a two-dimensional free energy surface $G(r,s)$ in the RX separation coordinate r and the solvent coordinate s, and again implement the theory for the model of the *t*-BuCl S_N1 ionization described in section 4 of part 1. We examine a wide range of solvent polarity, but often specialize to the three solvents considered in part 1: acetonitrile, chlorobenzene, and benzene.

In the usual conception of the S_N1 ionization, the reaction is pictured as the passage of the reaction system over a barrier in the RX separation r, and the transition-state theory (TST) would be applied to calculate the rate constant as k^{TST} for this process.[2] But as has been described generally for reactions in solution[3] and in particular for the S_N1 process by Zichi and Hynes,[4] and Lee and Hynes,[5a] this usual perspective involving TST assumes that equilibrium solvation holds; in particular, the solvent is supposed to remain completely equilibrated to the RX solute as the RX bond stretches and breaks, and its electronic charge distribution evolves, in the passage through the transition state. But this assumption is in general not valid: the time scale for the response of, e.g., the orientational polarization of the solvent is not sufficiently fast for the solvent to remain so equilibrated. In consequence of these nonequilibrium solvation conditions, the actual reaction path departs from the equilibrium path, and the rate constant differs from its TST approximation. (For general reviews of the extensive recent research on the departure from TST in

† Present address: Dept. of Chemistry, Carnegie Mellon Univ., Pittsburgh, PA 15213-3890.

(1) Kim, H. J.; Hynes, J. T. *J. Am. Chem. Soc.*, preceding paper in this issue.

(2) Ingold, C. K. *Structure and Mechanism in Organic Chemistry*, 2nd ed.; Cornell University Press: Ithaca, NY, 1969. Reichardt, C. *Solvents and Solvent Effects in Organic Chemistry*, 2nd ed.; Verlag Chemie: Weinheim, 1988. Entelis, S. G.; Tiger, R. P. *Reaction Kinetics in the Liquid Phase*; Wiley: New York, 1976.

(3) (a) van der Zwan, G.; Hynes, J. T. *J. Chem. Phys.* **1982**, *76*, 2993. (b) van der Zwan, G.; Hynes, J. T. *J. Chem. Phys.* **1983**, *78*, 4174. (c) van der Zwan, G.; Hynes, J. T. *Chem. Phys.* **1984**, *90*, 21. (d) See also: Hynes, J. T. In *The Theory of Chemical Reaction Dynamics*; Baer, M., Ed.; CRC Press: Boca Raton, FL, 1985; Vol. 4.

(4) Zichi, D. A.; Hynes, J. T. *J. Chem. Phys.* **1988**, *88*, 2513.

(5) (a) Lee, S.; Hynes, J. T. *J. Chem. Phys.* **1988**, *88*, 6863. (b) Lee, S.; Hynes, J. T. *J. Chem. Phys.* **1988**, *88*, 6853.

0002-7863/92/1514-10528$03.00/0